# Impact Analysis Of High Pressure Fragmentation


By

Kashif Zahir
NUST201361536MRCMS64213F

Supervisor
Dr.Salma Sherbaz

A thesis submitted in partial fulfillment of the requirements for
Master of Science
in
Computational Science and Engineering

Research Center for Modeling and Simulation
National University of Sciences and Technology

Feb 2017

# Approval

It is certified that the contents and form of the thesis entitled "**Impact Analysis of High Pressure Fragmentation**" submitted by **Kashif Zahir** have been found satisfactory for the requirement of the degree.

Advisor: **Dr. Salma Sherbaz**

Signature: _____
Date: _____

Committee Member 1: **Dr.Adnan Maqsood**

Signature: _____
Date: _____

Committee Member 2: **Dr.Zartasha Mustansar**

Signature: _____
Date: _____

Committee Member 3: **Dr.Ammar Mushtaq**

Signature: _____
Date: _____

# Dedication

To my Family for their Prayers without which I would not have been able to carry out my studies

# Certificate of Originality

I hereby declare that this submission is my own work and to the best of my knowledge it contains no materials previously published or written by another person, nor material which to a substantial extent has been accepted for the award of any degree or diploma at RCMS, NUST or at any other educational institute, except where due acknowledgment has been made in the thesis. Any contribution made to the research by others, with whom I have worked at RCMS, NUST or elsewhere, is explicitly acknowledged in the thesis. I also declare that the intellectual content of this thesis is the product of my own work, except for the assistance from others in the project's design and conception or in style, presentation and linguistics which has been acknowledged.

Author Name: **Kashif Zahir**

Signature: _____

# Acknowledgment

It was a great pleasure to work/study in NUST over the last two years and to be part of RCMS. The research work at RCMS, NUST has undoubtedly motivated me and has inspired my research. Therefore I would like to acknowledged everybody who contributed to the successful realization of this thesis, professors and colleagues, friends and family.

My deepest gratitude goes to my advisor, Assistant Professor Dr.Salma Sherbaz for her valuable guidance. Her great Enthusiasm and perpetual energy created a positive team work atmosphere, enhancing her advisee's creativity. Her involvement and original ideas have triggered and nourished my intellectual maturity that I will benefit from, for a long time to come.

I was delighted to work with Assistant Professor Dr.Adnan Maqsood during my stay in NUST. He was available, willing to Help and debate. His crucial contribution was a backbone of this research and Thesis.

I owe special acknowledgment to Assistant Professor Dr.Zartasha Mustansar, Assistant Professor Dr.Ammar Mushtaq, as my thesis committee members.

I am indebted to my colleagues for their support, stimulating scientific discussions and even more important, their overall good company. In particular, I would like to thank those who were patient when technical difficulties arose.

Finally, my friends and my dear family, I would not have been able to write this manuscript without you.

Thank you for your precious supports and Enthusiasm.

**Kashif Zahir**

# List of Abbreviation

| | |
|---|---|
| RDX | Cyclotrimethylenetrinitramine |
| TNT | TriNitroToluene |
| Comp B | Mixture of TNT and RDX |
| Tetryl | Trinitrophenylmethyinitramine |
| $B$ | Ballistic Coefficient |
| $G$ | Gurney Constant |
| PDF | Probability density function |
| CDF | Cumulative distribution function |

# Contents

# List of Figures

# List of Tables

# Abstract

Damage due to explosive is second to none amongst the threats faced by Pakistan. It's damaging not only the economy, political stability, social sector, but also national security and integrity. The threats from a conventional explosive based shell depend on two parameters, the charge weight and the distance between fragmentation point and the target. Materials used in explosive shells can be characterized on the basis of their nature as solid, liquid or gaseous. Unwanted blast events such as terrorist attacks with improvised explosive devices or unexploded ordnance accidents are a constant threat to our present-day society.

Injuries can be due to the energized fragments flying through the air and it can affect any part of the body. A profound understanding of this phenomenon is required for the estimation of potential hazards from the fragments generated by detonating ammunition items.

The fragment formation due to release of high energy from explosive shell is a random process and cannot be defined exactly. Therefore probabilistic approaches are generally used for the assessment of fragment and their hazards. The fragments produced from the detonation of a single shell can be characterized by their fragment numbers with respect to fragment mass, and initial velocity.

The basis of this research is to estimate the terminal impact of fragments produced in 2-D and 3-D fragmentation of cylindrical shell. Statistical formulation is used for estimation of fragment mass in both cases. Fragment trajectories under the action of constant drag and Gravity are calculated from three dimensional equations of motion.

Fragmentation of explosive shell depends on number of factors, like geometric shape and size, angle of attacked. In this study a fragment throw model which consider the drag, area, mass and air density as input parameters is used to predict the flight trajectory of fragments. To analyze the terminal impact, range and dispersion of different types of fragments, probabilistic modeling is used. We used Mott Distribution for 2-D and 3-D fragments masses. The final deliverable is the development of a generic frame work, the dispersion graphs and probability damage at three different positions.

# Chapter 1

# Fragmentation

## 1.1 Introduction

Fragmentation is the disintegration of a contiguous body into several pieces. Dynamic fragmentation depends on mechanical properties of the material used with a strong dependence on time. This phenomenon occurs at various scales and at multiple extents in nature. For example at astrophysical scale, a supernova is the largest explosion that takes place in space, generating fragments of various scales. Supernova are among the most powerful and spectacular events in the universe. It is the biggest explosion one can imagine, the brilliant, dying gasp of a star that is at least five times more massive than our sun. Similarly a glowing fragments of rocks matter, known as meteorites burn and glow upon entering the earth's atmosphere. At smaller scales, DNA fragmentation controls cell replication [1], nuclear and elementary particle collisions constantly occur in daily life [2]. Fragmentation due to bird strikes during takeoff or landing of an aircraft, car crashes and glass breakage are important concerns in the field of Structural Engineering.

Moreover in nuclear power plants, concrete structures are designed to resist extreme loadings. In the military domain, deeper understanding of physics behind dynamic fragmentation is important for strengthening tanks and bullet-proofing for army personal. The fragmentation also concerns the medical industry a useful technique for the removal of kidney stones without surgical procedure (by sending pressure pulses onto the stone to break it into smaller pieces), which may then be removed naturally. In crushing and milling operations, fragmentation control through effective blast design is a challenging task for Engineers [3].

A meteor exploded in the sky over Chelyabinsk on Feb 15 2013, in southern Rus-

sia. The explosion cause no damage to human and infrastructure, but the shock wave injured about 1500 people and damage around 7200 building in the surrounding region. Though Chelyabinsk meteorite, weighting about 12,000-13,000 metric tonnes and $17 - 20m$ in diameter before it exploded, scientist claim that it is very small compared to other meteorites that could possibly hit the earth surface. The released energy estimated from Chelyabinsk explosion is about 500 Kilotons of TNT [4]. In the past, falling meteorites have also caused damage to property and life.

- September 29, 1938 - a small meteorite crashed the roof of a garage in Benld, Illinois.
- November 30, 1954 - a $4kg$ meteorite fell through the roof of a house and damaged Ann Hodges, in Sylacauga, Alabama.
- October 09, 1992 - a $12.7kg$ meteorite demolished a car near New York City.
- September 23, 2003 - a $20kg$ meteorite hit a 2 story house in New Orleans, Louisiana.
- September 28, 2003 - a cluster of meteorites damaged several houses and injured 20 people in Odisha, India.

The space fragments (debris) poses a collision hazard to operational satellites in geocentric orbits [5]. Owing to their high velocities (up to $17,500mph$), even very small size space fragments can damage a satellite or even a spacecraft [6].

## 1.2 Explosion Based Fragments

The explosion is a physical phenomenon that results in a large scale, rapid and sudden release of energy. The characterization of this phenomenon is based on its nature, i.e physical, nuclear or chemical. The physical explosion is a sudden release of high level energy due to failure of a compressed gas cylinder, on mixing of two chemicals at different temperatures or volcanic eruption. The eruption of Krakatoa volcano in 1883 is an example of physical explosion. A large amount of molten lava was spilled into the ocean during this eruption resulting the vaporization of about 1 cubic mile of sea water and creating a blast wave which could be heard from a distance of 3000 miles [7].

A nuclear explosion is a rapid release of energy from a high-speed nuclear reaction.

The underlying reaction can be fission, fusion or a multistage cascading combination of the both. In nuclear fission reaction, when a neutron collides with a nucleus of a large atom, it forms two or more smaller nuclei releasing energy and neutrons. The neutrons then trigger further fission, and so on. In a nuclear fusion reaction, a pair of light nuclei unites together to form a nucleus of heavier atom. It is important to point out that an explosion at a nuclear power plant is also possible. Any nuclear explosion can be widespread, long lasting and catastrophic effects [8]. In the chemical explosions, rapid oxidation of fuel elements is the main source of energy.

Explosive materials can be characterized as solid, liquid or gases. Blast effects are best known in the case of solid explosives. Another parameter to classify the explosive material can be their sensitivity to ignition as primary and secondary. Materials such as mercury fulminate and lead azide are primary explosives. Secondary explosive when detonated create blast waves which can result in widespread damage to the surroundings. Materials such as TNT and RDX are secondary explosive [9].

Energy release spectrum of an explosion with respect to time is very wide ranging from below a microsecond to seconds, Figure 1.2. The shortest times are normally related to condensed phase detonations and pressure vessel ruptures, whereas the longest times are linked to combustion explosions. The maximum pressure developed from an explosion follows the same pattern, Figure 1.1. The highest peak pressures usually associated with nuclear weapons and conventional explosives [10].

The difference between the ambient pressure and explosion pressure is called over-pressure, Figure 1.3. The strength of over-pressure blast wave decreases with increasing the distance from center of the fragmentation point. Both the positive and negative overpressure from the blast can cause serious damage to structures, people, and other objects.

The thermal impact is another important effect of an explosion and it occurs when a fireball, or a volume of hot gases is generated in a combustion or nuclear explosion. When a structure, generally close to the center of fragmentation point is engulfed by a fireball, thermal effects are primarily from radiant heat transfer from the fireball and convective heating of structures. In normal cases, the thermal effects might not be as important as those from overpressure and fragment, but in the situation where the over-pressure and fireball effects damage the fire-resisting system of the structures, intense heat can weaken the structural coating. This can result in the failure of those structure, leading to a localized or progressive collapse. The World Trade Center attack on 9/11 is an example of such an instance. Thermal energy can also injure people, and ignite various objects in a structure such as furniture. Fireball created

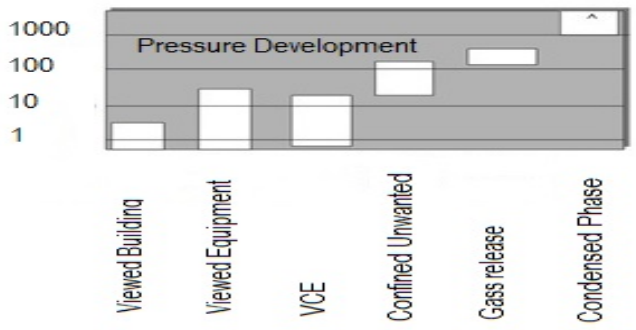


Figure 1.1: Pressure Development peak(psi) [10]

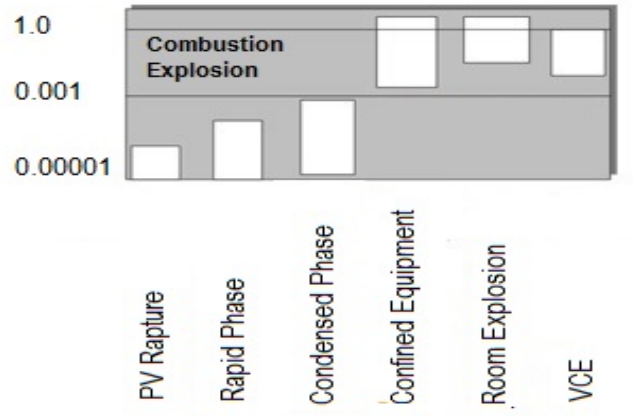


Figure 1.2: Energy Release time scales(sec) [10]

from an explosion, can cause significant damage [13].

Projectiles consist of fragments and fragment is an object which was originally at some distance from the fragmentation point and is flung by the expanding pressure wave and wind produced by the explosion Figure 1.5.

The fragments usually follow a parabolic path through the air, Figures 1.4. The damage caused by these fragments depends on their initial velocity, the distance between the point of fragmentation and target, the angle of obliquity (angle the fragment strikes target), the physical properties of fragments and the target. High energy fragments can cause significant harm to structures and people which they strike.

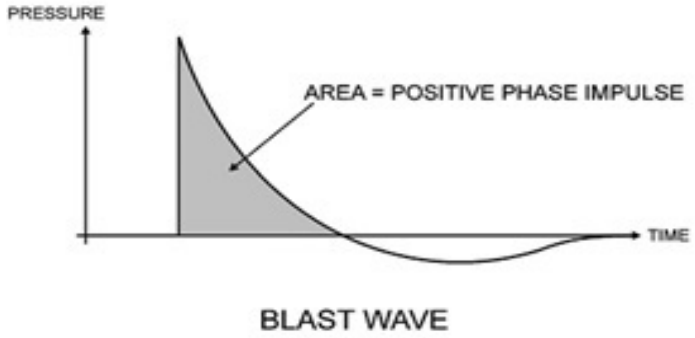


Figure 1.3: Blast Wave [9]

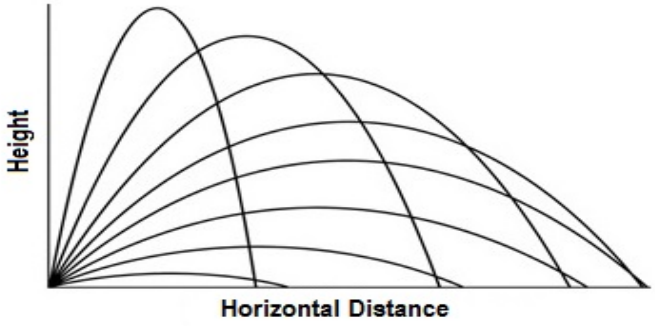


Figure 1.4: Illustrative Trajectories of Fragments

Depending on the location, cratering and ground shock, damage can also be the possible outcomes of an explosion. If on or close to the ground, a tremor is transmitted over a distance by the ground; which is excavated locally [14]. The strength of cratering is associated with the soil type and blast location. The tremor can result in the damage to a structure's foundation, whereas cratering fragments can cause significant harm to the structure and bystanders.

## 1.3 Fragments Impact on Human Body

The blast injuries are generally divided into four categories, i.e. primary, secondary, tertiary, and quaternary. Secondary blast injuries are due to the energized fragments flying through the air and can affect any part of the body. A brief overview of four

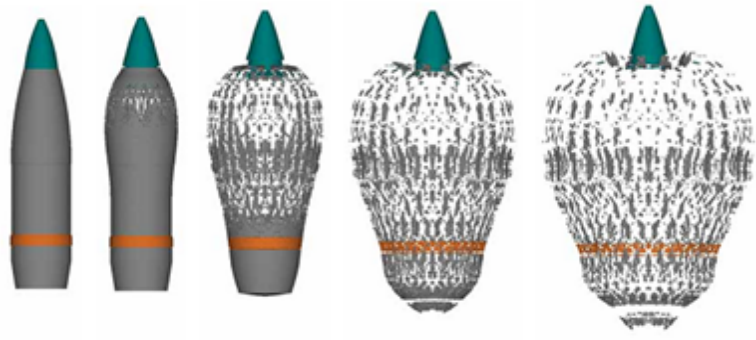

Figure 1.5: Fragmentation of 105 mm HE Projectiles casing [11]

categories of blast injuries is given in Table below[15, 16].

| **Primary Blast** | |
|---|---|
| Characteristics. | |
| Associated with high explosives (HE), occurs as an overpressure blast waves that move through body | Body parts affected: The most vulnerable organs to this type of blast are ears, lungs, and gastrointestinal tract. |
| **Secondary Blast** | |
| Characteristics: | |
| Results from flying debris and shell fragments | Body parts affected: Any body part can be affected. |
| **Tertiary Blast** | |
| Characteristics: | |
| Occurs when individuals are thrown by the blast wind | Body parts affected: Skull (closed and open brain injuries) and long bone fractures |
| **Quaternary Blast** | |
| Characteristics: | |
| Includes all other injuries like burns (chemical or thermal); Injuries due to structural collapse; and toxic dust, gas, or radiation exposure | Body parts affected: Any body part can be affected |

## 1.4 Fragmentation Modeling and Associated Challenges

Explosives materials are used in various types of ammunitions like missiles and bombs. Unwanted blast events such as terrorist attacks with improvised explosive devices are a constant threat to our present-day society. A profound understanding of the possible damage is required for the reduction of potential impact of such events/accidents.

Owing to the inherent complexity and the degree of randomness involved in the phenomenon of fracture of case metal surrounding the bursting charge, the investigation of fragment effects requires a probabilistic approach. Due to the random nature of the breakup of case metal, terminal ballistic parameters such as the impact distance and velocity also exhibit statistical variations.

## 1.5 Objective and Scope of Work

The key objective of this research is to estimate the terminal impact of resultant fragments, range and dispersion. Mott formulation is used for estimation of 2-D and 3-D fragments mass distribution. Fragment trajectories under the action of constant drag and Gravity are calculated from three dimensional equations of motion.
The scope of research includes.

A limited parametric study is performed to estimate the risks of human injury from fragmentation of cylindrical shells, by considering.

- Various explosive types
- Different shell thickness

## 1.6 Organization of Thesis

Thesis is divided into Six chapters. A brief description of each chapter is given below

- Chapter one is a formal description of fragmentation theory. It consist of basic of fragmentation, then its applications in science and engineering,

- Chapter two is a collection of pioneer formulations in the area of fragmentation are elaborated.
- Chapter three provides the details of mathematical models used for the estimation of potential hazard from the fragments generated by detonating ammunition items on the potential explosion site.
- Chapter four presents the results of 2-D fragmentation of a cylindrical shell. The important parameters (number and mass distribution of fragments and the initial velocity) required to estimate the risks of human injury due 2-D fragmentation of a cylindrical shell, are calculated.
- Chapter five presents the results of 3-D fragmentation of a cylindrical shell .
- Chapter six deals with the significant conclusions of current research work and recommendation for future work.

.

# Chapter 2

# Literature Review

## 2.1 Background

Fragmentation has appealed to researchers from different areas. Physicists, statistician, Mechanical and Civil Engineers formulated several models to study the breakage of a structure subjected to high pressure. First empirical formulation concerning fragmentation was proposed in 1933. This chapter is divided in three sections. In the first section, pioneer empirical formulations in the area of fragmentation are elaborated. The seconds and third section deal with the analytical models and physics-based models respectively. The analytical models are based on statistical and geometrical arguments whereas physics-based models explain how energetic and dynamic arguments lead to complex principles.

## 2.2 Empirical Formulation

### 2.2.1 Rosin and Rammler Formulation

Rosin and Rammler's [17] while working in coal and ore crushing industry, provided the first empirical description of fragmentation. They predicted fragment size distributions by sorting out fragments in different size ranges, using a collection of sieving screens. Later, in 1939 Weibull suggested a similar distribution, which he obtained by analyzing the fracture of materials under repetitive stress. Rosin-Rammler's distribution is given by.

$$F(x) = 1 - e^{-(x/xo)^{\beta}} \tag{2.1}$$

where $xo$ is the characteristic fragment size and $\beta$ is shape distribution.

### 2.2.2 Schuhman Law

The Gates-Gaudin-Schuhmann distribution [18], a limiting form of Rosin and Rammler's distribution, is generally used to evaluate the particle size distribution data in communication processes [19, 20, 21, 22]. It is a two parameter distribution function which follows a power law and is given by.

$$F(x) = e^{-(x/xo)^{\beta}} \tag{2.2}$$

Schuhmann distribution [18] which is define in forties has been used since seventies to pinpoint that fragmentation is repetitive in nature. The concept of repetition (self-similarity) has appealed to many scientists and engineers.

### 2.2.3 Mott and Linfoot Formulation

At the time of World War II, NF Mott, a Nobel Laureate in Physics [23] formulated the fragments mass distribution for the data obtained through explosive rupture of cylindrical bombs.

$$F(x) = 1 - e^{-(m/mo)^{1/2}} \tag{2.3}$$

where $m$ is the fragment mass, and $mo$ is a characteristic mass. Mott and Linfoot did a great deal of research on the fragmentation and constitute the basis for much of the current research [23, 24].

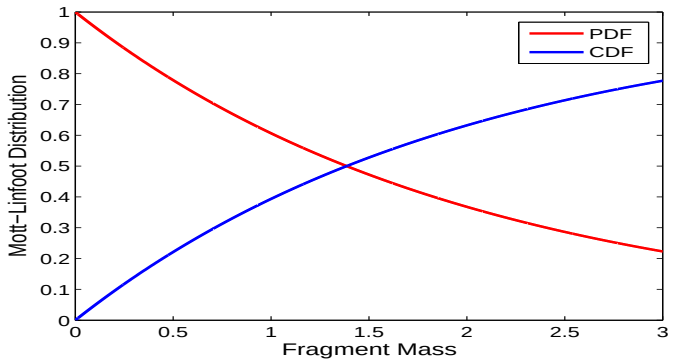


Figure 2.1: Moot Linfoot Distribution [23, 24]

## 2.3 Geometrical Formulation

### 2.3.1 Lineau Theoretical Formulation

Lineau [25] modeled fragmentation as the random geometric fracture of an infinite one-dimensional body. He considered a line of infinite length that is about to break-down into several fragments. Since each point along the line has equal probability of being a breakpoint, length of the fragments was determined statistically from randomly-placed breakpoint.

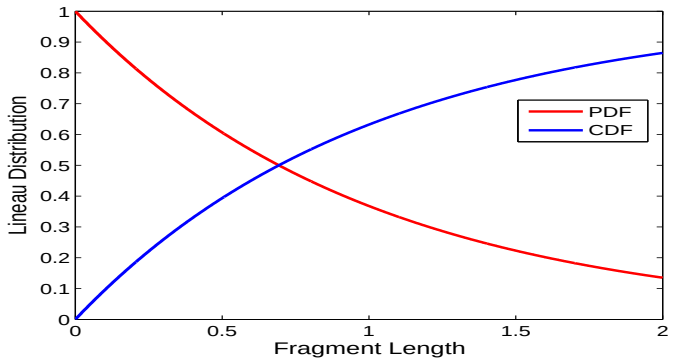


Figure 2.2: Lineau Distribution [25]

If we randomly introduce the breakpoints in a line then sequence of failure will follow a Poisson point statistics and the probability of $k$ breakpoints within a given length $l$ will be given by.

$$p(k,l) = \frac{\left(\frac{l}{lo}\right)^k e^{(l/lo)}}{k!} \tag{2.4}$$

Where $lo$ is the average space between the breaks. The probability of occurrence of fragments of length $l$ within time difference $dl$ is.

$$f(l)dl = P(0,l)P(1,dl) = (1/lo)e^{(l/lo)}dl \tag{2.5}$$

$f$ is the probability density function associated with the process, by integrating it we can calculate the cumulative density function [32].

$$F(l) = 1 - e^{-(l/lo)} \tag{2.6}$$

### 2.3.2 Binomial Theoretical Formulation

In case of line of finite size $L$, then the poison point statistics is not applicable for randomly place breakpoints. Binomial probability is applicable in case of finite size $L$.

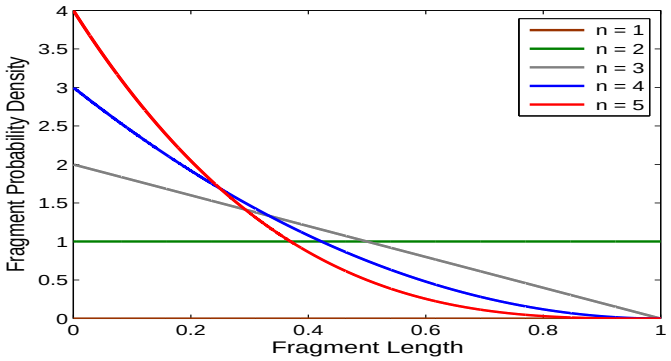


Figure 2.3: Poisson Distribution

The cumulative distribution is

$$F(l) = 1 - \left(1 - \frac{1}{L}\right)^{Nf-1} \tag{2.7}$$

Where $Nf$ is the number of fragment. When become large binomial distribution converge to Lineau Distribution.

### 2.3.3 Voronoi-Dirichlet's Formulation

Voronoi-Dirichlet's Formulation has extensively applied in diverse fields such as natural sciences, mathematics, as well as computer science. Voronoi-Dirichlet's has been employed in analysis of giraffe skin and honeycomb, cosmology [27], climate modeling[28], in crystallography[29], and fracture mechanics[30]. Two dimensional construction begins with a random placement of points on the plate, Space is then discretized by construction of orthogonal bisecting lines.

#### 2.3.3.1 One Dimension Formulation

Voronoi-Dirichlet's formulation is the dual of the Lineau formulation. Lienau's points represent breakpoints, whereas in Voronoi-Dirichlet's formulation they are center of fragments. The probability of finding a length $l$ is given by poison point process is.

$$f(l)dl = (1/lo)e^{-(l/lo)}dl \tag{2.8}$$

The probability of finding a length $l_1$ adjacent to a length $l_2$ is

$$f(l_1)f(l_2)dl_1dl_2 = (1/lo^2)e^{-(l_1+l_2)/2}dl_1dl_2 \tag{2.9}$$

By applying the transformation $L = (l_1 + l_2)/2$ and $\psi = (l_1 - l_2)/2$

$$f(L) = \frac{2}{lo}\frac{2}{lo}e^{-(2L/lo)} \tag{2.10}$$

#### 2.3.3.2 Multi-Dimensional Formulation

Equation above is the gamma function with shape parameter 2. Kiang [31] show that symmetrical high order gamma function provide fragment size distributions for Voronoi-Dirichlet's formulation. The general expression of the fragment distribution as a function of the fragment mass is

$$f(m) = \frac{1}{mo}\frac{n}{\Gamma(n)}\left(\frac{nm}{mo}\right)^{n-1} e^{(-nm/mo)} \tag{2.11}$$

Where $m$ is the fragment mass and $n$ is the dimension parameter with values 2, 4, 6. Value of 2 for a line, 4 for surface, 6 for volume. More information can be found in[34]

### 2.3.4 Grady-Kipps Formulation

Grady and Kipps [32] find that Mott and Linfoot distribution which is studied for exploding steel cylinders is not necessarily give the best fitting distribution in multiple dimensions. They observed that Lineau formulation is binomial in one dimension, fragmentation in two and three dimension follow poisson point process. Despite difference with the Mott and Linfoot distribution, Grady and Kipps keep the same linear exponential function for both area and volume.

$$F(s) = 1 - e^{-(s/so)} \tag{2.12}$$

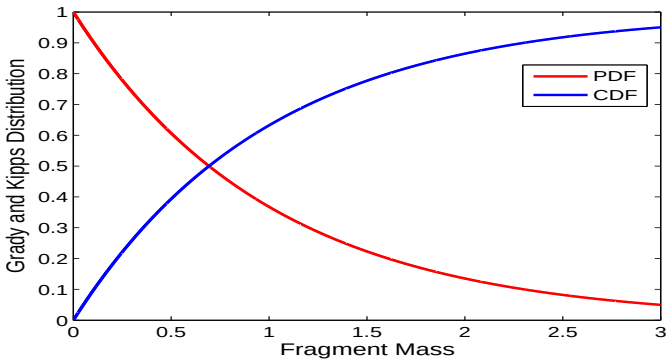


Figure 2.4: Grady Kipps Distribution [26, 32]

### 2.3.5 Modification of Mott Formula

#### 2.3.5.1 Mott Formula

Natural Fragmentation of shells results in a wide range of fragment size. Different authors suggested several formulae for the prediction of fragments size, the one best known is probably the Mott Formulae.

$$N(m) = \frac{M_0}{2{M_k}^2} exp(-m^{1/2}/M_k) \tag{2.13}$$

Where $N(m)$ is the number of fragments with a mass greater than $m$. $M_0$ is the total mass of fragments, $M_k$ is a parameter characterizing the fragment mass distribution which can be estimated as

$$M_k = Bt^{5/6}{d_i}^{1/3}(1 + t/d_i) \tag{2.14}$$

Here $B$ is a constant depending on the explosive type, $t$ is the thickness and $d_i$ is the internal diameter of the warhead.

#### 2.3.5.2 Modified Mott Formula

For fragments of considerable size the Mott Formula give a fair estimate of fragment size. However the Mott did not provide an upper limit of fragment size.

There are numerous possible modifications [35] which will account for a maximum fragment size. we have the following to be the most promising one.

$$N(m) = \frac{\mu_0}{2{\mu_k}^2}\left(1 - sin\frac{\pi}{2}\frac{m}{m_{max}}\right)exp(-m^{1/2}/\mu_k) \quad \text{for} \quad m < m_max \tag{2.15}$$

$$N(m) = 0 \quad \text{for} \quad m > m_max \tag{2.16}$$

Here three parameters are used to describe the size distribution. $\mu_0$ it must be chosen so that total mass of fragments is equal to Mass of casing. $\mu_k$ it can not be estimated from an equation like Eq 2.15, but has to be determined from experimental data. $m_{max}$ it must be estimated from an experimental data.

## 2.4 Sequential Fragmentation

The problem of characterizing the distribution of particles from fragmentation experiments always approached empirically. Ideally it is possible to derive the desire analytical distribution from a physical theory of fragmentation. Wilbur K. Brown [36] present his own work of sequential fragmentation with the following foam.

$$n(m) = c\int_m^\infty n(m')f(m'\rightarrow m)dm' \tag{2.17}$$

Here $n(m)$ is the number of particle distribution with dimensions for the number of fragments per unit mass of mass between $m$ and $m + dm$.

The function $f(m'\rightarrow m)$ describe the mass distribution that results when a single

fragment of mass $m'(> m)$ break up into lighter pieces.

$$f(m' \rightarrow m) = \left(\frac{m}{m_1}\right)^{\gamma} \tag{2.18}$$

$\gamma$ is a free parameter ($-1 \leq \gamma < 0$), and $m_1$ is mass related to average fragment mass in the distribution $n(m)$.
when we insert equation 2.18 into 2.17 we obtained the following 2.19

$$n(m) = \left(\frac{m}{m_1}\right)^{\gamma} \int_m^{\infty} n(m') d\left(\frac{m'}{m_1}\right) \tag{2.19}$$

For $(-1 < \gamma < 0)$

$$n(m) = \frac{N_T}{m_1}\left(\frac{m}{m_1}\right)^{\gamma} exp\Big[ - \frac{(m/m_1)^{\gamma+1}}{\gamma+1}\Big] \tag{2.20}$$

Normalized Expression is

$$\int_0^{\infty} n(m) dm = N_T \tag{2.21}$$

For special case $\gamma$ = -1

$$n(m) = K\left(\frac{m}{m_1}\right)^{-1} \tag{2.22}$$

where $K$ is constant (total number of fragments,$N_T$ is undefined in this case)
The sequential fragmentation mass distribution for $(-1 < \gamma < 0)$ is

$$mn(m) = N_T \left( \frac{m}{m_1} \right)^{\gamma} exp\left[ - \frac{(m/m_1)^{\gamma+1}}{\gamma + 1} \right] \tag{2.23}$$

and for $\gamma$=-1

$$mn(m) = Km_1 \tag{2.24}$$

### 2.4.1 Fragment Mass Distribution of Naturally Fragmenting Warheads

As the modeling of fragmentation process is of utmost important for design, redesign and efficiency analysis. The fragment mass distribution along with the initial velocity, the spatial and shape distribution of fragments, enable the complete characterization of fragmentation process.

Natural fragmentation of HE projectile is the result of complex process of explosive detonation, gas products expansion and behavior of casing material under intense impulse loads. Having in mind the complexity of underlying physics the semi-empirical based approach seems to be a promising one to the fragment mass distribution.

Fragment mass distribution is usually describe by a cumulative distribution function rather than a probability density function which is more sensitive to the scatter of fragment mass data. The cumulative numbers of fragments $N_T(m) = N_T(> m)$ with the mass greater than m and alternatively, the cumulative fragment mass $M_T(m) = M_T(> m)$ is the total mass of all fragments with individual mass greater than m.

$$N(m) = \frac{N_T(m)}{N_0}, \qquad M(m) = \frac{M_T(m)}{M_0} \tag{2.25}$$

Where $N_0$ is the total number of fragments and $M_0$ is the total mass of fragments. The relation between cumulative distribution is.

$$\frac{dM}{dm} = \frac{m}{\overline{m}} \frac{dN}{dm} \tag{2.26}$$

Distribution mean which is most important characteristics is determined by

$$\overline{m} = \frac{M_0}{N_0} = \int_0^\infty N(m) dm \tag{2.27}$$

A very useful numerical property of distribution is Median which is define by

$$N(\tilde{m}_N) = \frac{1}{2}, \qquad M(\tilde{m}_M) = \frac{1}{2} \tag{2.28}$$

There are numerous distribution laws that are used to describe a real distribution of HE Projectile fragments.

#### 2.4.1.1 Generalized Mott Distribution

Mott [23] urged that in three dimensional fragmentation of thick walled cylinder, where fragments do-not retain the inner and outer surface of original cylinder.

Mott formulate this procedure in the form of distribution by using the relation

$$N(m) = exp\left[ - \left( \frac{m}{\mu} \right)^{\lambda} \right] \tag{2.29}$$

This distribution correspond to two parametric Weibull Distribution

#### 2.4.1.2 Generalized Grady Distribution

Grady and Kipp's [34] formulate simple linear exponential distribution and is given by

$$N(m) = exp\left[ - \left( \frac{m}{\mu} \right) \right] \tag{2.30}$$

Later on, this distribution is extended to other dimension and name as Generalized Grady Distribution which is given by

$$N(m) = fexp\left( - \frac{m}{\mu_1} \right) + (1 - f)exp\left( - \frac{m}{\mu_2} \right) \tag{2.31}$$

#### 2.4.1.3 Log-normal Distribution

On the multiplicative nature of fragmentation process several authors suggest log normal distribution for describing the fragment mass distribution[37, 38].

$$N(m) = \frac{1}{2}\left[ 1 - erf\left( \frac{lnm - \mu}{\sqrt{2}\sigma} \right) \right] \tag{2.32}$$

Where $erf(.)$ is error function $erf(x) = \frac{2}{\sqrt{\pi}} \int_0^x e^{-t^2} dt$

#### 2.4.1.4 Weibull Distribution

The two parametric Weibull distribution [37], which is originally used for the description of grain size distribution in grinding process is redefine as.

$$M(m) = exp\Big[ - \left(\frac{m}{\mu}\right)^{\lambda} \Big] \tag{2.33}$$

# Chapter 3

# Mathematical Model

The fragmentation and fragment formation due to the explosion of an ammunition is a random process and cannot be defined exactly. Therefore probabilistic approaches are generally used for the assessment of fragment and their hazard. The fragments produced from the detonation of a single weapon can be characterized by fragment numbers with respect to fragment mass, and their initial velocity.

The details of mathematical model used for the estimation of potential hazard from the fragments generated by detonating ammunition items in the Potential Explosion Site (PES), are given in following paragraphs.

## 3.1 Fragment Mass Distribution

The fragment mass data is represented in the form of the cumulative distribution for the number of fragments $N_T(m) = N_T(> m)$ with the mass greater than $m$. Generalized Mott distribution is used in the current study

### 3.1.1 Generalized Mott Distribution

Predrag Elek and Slobodan Jaramaz [37, 38] redefine well known Mott Distribution as a Generalized Mott Distribution for different dimensions

$$N(m) = e^{-\left(\frac{m}{\mu}\right)^{\frac{1}{\lambda}}} \tag{3.1}$$

Where $N(m)$ is the total number of fragments with the mass greater than $m$, $\mu$ is mean fragment mass and estimated by the formula

$$\mu^{1/2} = Bt^{(5/6)}d^{(1/3)}\left(1 + \frac{t}{d}\right) \tag{3.2}$$

Where $t$ is the thickness of casing, $d$ is the diameter of casing and $B$ is the constant and is specific for a given explosive-metal pair. Distribution Mean used in the Mott fragmentation model is $2\mu$ and $6\mu$ for 2-D and 3-D respectively.

## 3.2 Initial Velocity

The formula given by Gurney[39] is used for estimating the initial velocity for each fragment. Gurney constant $G$ has specific values for a given explosive type derived experimentally

$$V = GR^{\left(\frac{1}{2}\right)} \tag{3.3}$$

and $R$ is define as

$$R = \left[\frac{m_1}{m_2 + 0.6m_1}\right] \tag{3.4}$$

Where $m_1$ is the explosive mass and $m_2$ is the casing mass.

Table 3.1: Values of $B$ and $G$ for Four Explosive [40]

| $Constant Values$ | | |
|---|---|---|
| Explosive | $B\left(\frac{kg^{1/2}}{m^{7/6}}\right)$ | $G\left(\frac{m}{s}\right)$ |
| Comp B | 2.7026 | 2,774 |
| RDX | 2.5809 | 2,926 |
| TNT | 3.3113 | 2,499 |
| Tetryl | 3.7983 | 2,438 |

## 3.3 Fragments Projected Area

If we assume that the fragments generated by a given explosive material are geometrically similar, then mass $m$ and presented area $A$ are related by the shape factor $k$.

$$M = kA^{3/2} \tag{3.5}$$

The values of shape factor or ballistic density $k$ are calculated empirically from ballistic tests for a given weapon. In case of forged steel projectiles the average value of $2.60g/cm^3$ has been recommended [12, 11].

## 3.4 Drag

Any object moving through the air will experience drag, a force due to pressure and shear stress on the surface of an object in the direction of flow. This force is a combination of normal and tangential forces on the body.

Information pertaining to drag on different objects is a result of numerous experiments with wind, water tunnels, and other ingenious devices that measures the drag on scale models. These measured values put in dimension less form.

$$C_D = D/(0.5AU^2\rho) \tag{3.6}$$

The drag $D$ acting on a fragment follows the velocity-squared law and is proportional to the product of square of the velocity $U$ and mean presented area $A$.

where $C_D$ is a function of dimension less parameters such as Reynold Number ($Re$), Mach Number ($Ma$), Froude Number ($Fr$), and relative roughness of the surface, $\epsilon/l$.

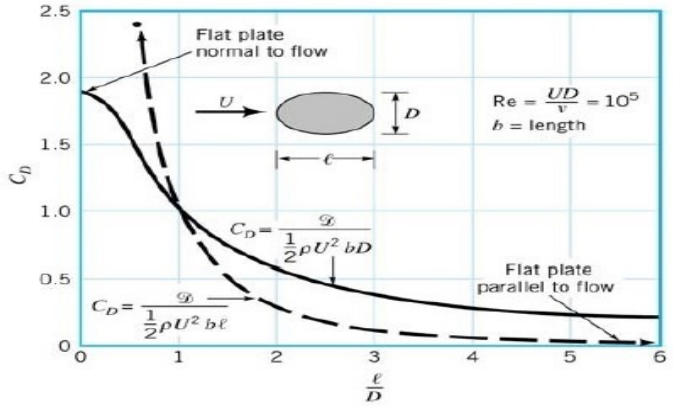


Figure 3.1: Drag Coefficient [41]

$$C_D = \phi(shape, Ma, Re, Fr, \epsilon/l) \tag{3.7}$$

### 3.4.1 Shape Dependence

The dependence of the drag coefficient on the shape of object is shown in Figure 3.1. Drag on an ellipse can be illustrated with aspect ratio $l/D$, Where $D$ is the thickness and $l$ length parallel to the flow. With $l/D = 0$ we obtained the flat plate value of $C_D = 1.9$. With $l/D = 1$ the corresponding value of $C_D = 1$. As the value of $l/D$ increases the value of Drag coefficient decreases [41].

Since It is difficult to calculate the drag coefficient of irregular fragments, a useful approximation [42] is to take the drag coefficient value of 1.21.

## 3.5 Trajectory Analysis

Fragment trajectories under the action of drag and gravity forces are calculated using the equations,[42].

$$m\frac{d^2x}{dt^2} = -\frac{1}{2}A\rho C_D V\frac{dx}{dt} \tag{3.8}$$

$$m\frac{d^2y}{dt^2} = -\frac{1}{2}A\rho C_D V\frac{dy}{dt} - mg \tag{3.9}$$

$$m\frac{d^2z}{dt^2} = -\frac{1}{2}A\rho C_D V\frac{dz}{dt} \tag{3.10}$$

Where $A$ is the presented area of the fragment, $C_D$ is the drag coefficient $\rho$ is the density of air, $g$ is the acceleration due to gravity and $V$ is the instantaneous velocity.

$$V = \sqrt{\left(\frac{dx}{dt}\right)^2 + \left(\frac{dy}{dt}\right)^2 + \left(\frac{dz}{dt}\right)^2} \tag{3.11}$$

ODE45 technique has been used to solve these coupled nonlinear trajectory equations on the interval $\theta$ ( 0° - 360° ) and $\phi$ from ( 0° - 180° )

### 3.5.1 Probability of Damage Estimator

Depending on distribution, Areal Density $q$ of fragments on a surface away from the fragmentation point[11] is

$$q = \frac{Q_0}{4R^2}e^{\sqrt{2\frac{m}{m_0}}} \tag{3.12}$$

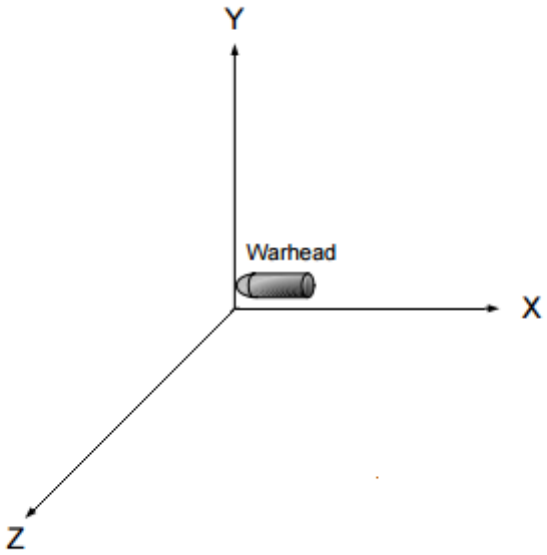


Figure 3.2: Coordinate System

where
$Q_o$ = Total Number of Fragments
$m_0$ = Mean Fragment mass
$R$ = Radius
$m$ = Fragment Mass

$$Damage \quad probability = 1 - e^{-qA_T} \tag{3.13}$$

where $A_T$ area of Human at Different postures [43].

Table 3.2: Values of Area for Three Posture.

| $AreaValues$ | | |
|---|---|---|
| $Index$ | $Posture$ | $Area$ |
| 1 | Standing | $0.58m^2$ |
| 2 | Assaulted | $0.37m^2$ |
| 3 | Supine | $0.10m^2$ |

# Chapter 4

# 2-D Fragmentation of Cylindrical Shells

Fragmentation of projectiles or warheads produces the fragments of different masses and geometries. These explosion based fragments are expected to cause severe damage to the human body at a certain distance. The important parameters required to estimate the risks of human injury from fragments of cylindrical shells include, number and mass distribution of fragments, geometrical shape, the initial velocity and their spatial distribution. In this chapter, the results of 2-D fragmentation of a cylindrical shells are presented. The details of the study are given in following paragraphs

## 4.1 Parameters of Explosive Munitions

Natural fragments spatial distribution (including their masses and geometrical shapes) is a complex function of internal and external geometry of the warhead case surface, mechanical properties of the warhead case (tensile strength and yield strength) and energetic characteristics of the explosive. The properties of explosive munitions used for the 2-D fragmentation analysis of cylindrical shells are shown in Table 4.1. A limited parametric study is performed to estimate the risks of human injury from fragments, considering

- Various explosive types
- Different shell thickness

Table 4.1: Parameters of Cylindrical Shell

| *Shell Parameters* | | |
|---|---|---|
| No | Parameter | Values |
| 1 | Shell length | $1.5400m$ |
| 2 | Shell mass | $136.5kg$ |
| 3 | Shell diameter | $0.2740m$ |
| 4 | Shell thickness | $0.2m, 0.15m$ |
| 5 | Explosive mass | $87.1kg$ |

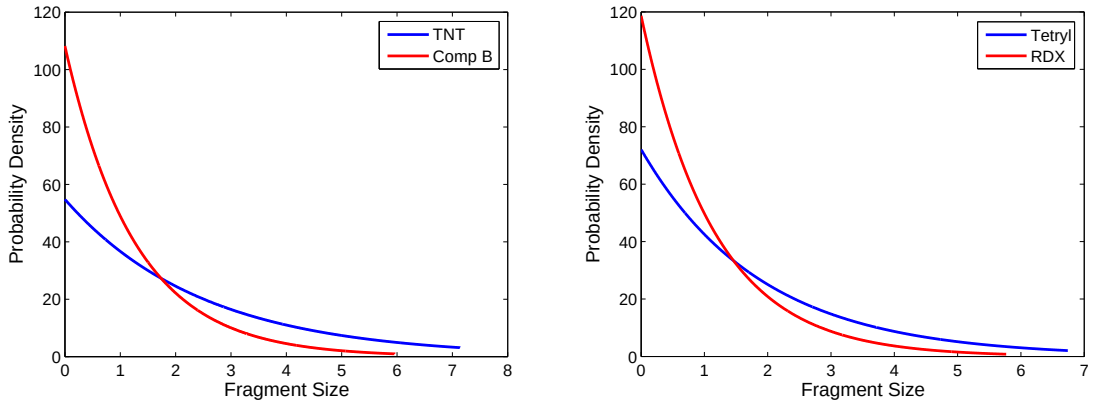


(a) Comp B,TNT (b) RDX,Tetryl

Figure 4.1: Fragmentation Pattern for 2-D Mott Distribution with Thickness of $0.2m$

## 4.2 Fragments Characteristic Parameters

### 4.2.1 Number and Mass Distribution of Fragments

2-D fragmentation of cylindrical shell produces the fragments of uniform thickness. The Mott formula (equations 3.1 and 3.2) are used for estimation of fragmentation number and mass distribution.
Figure 4.1 show fragmentation pattern based on 2-D Mott Distribution for shell with a thickness of $0.2m$. The total number of fragments generated, are estimated to be 108, 55, 119 and 72 for Comp B, TNT, RDX and Tetryl explosive materials respectively. It can be observed that in all four cases light fragments are produced in large numbers. The largest mass in case of Comp B and TNT are $5.9622kg$ and $7.1396kg$

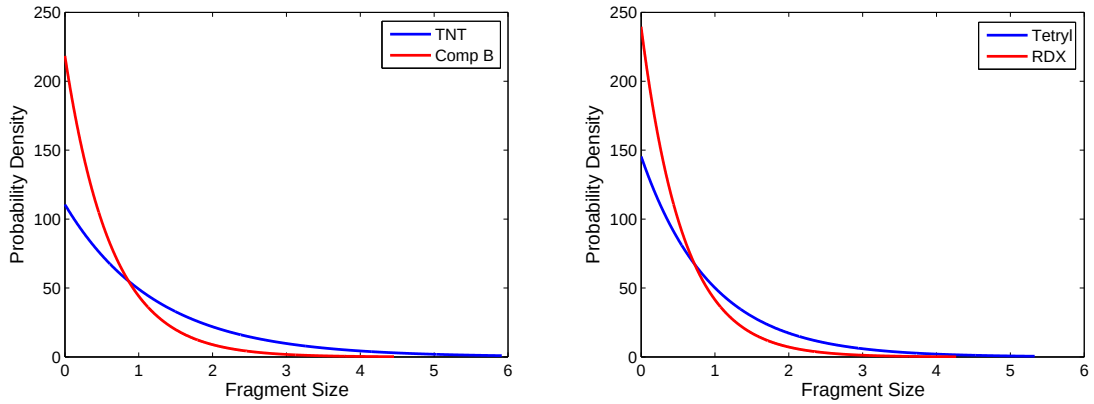


(a) Comp B,TNT (b) RDX,Tetryl

Figure 4.2: Fragmentation Pattern for 2-D Mott Distribution with Thickness of $0.15m$

respectively. As these are largest mass values, all fragments have mass smaller than $5.9622kg$ for Comp B and $7.1396kg$ for TNT.
Largest mass in case of RDX and Tetryl for a thickness of $0.2m$, are $5.7682kg$ and $6.7415kg$ respectively. As these are largest mass values, all fragments have mass smaller than $5.7682kg$ for RDX and $6.7415kg$ for Tetryl.

Figure 4.2 show fragmentation pattern based on 2-D Mott Distribution for shell with a thickness of $0.15m$. The total number of fragments generated, are estimated to be 218, 111, 240, and 146 for Comp B, TNT, RDX and Tetryl explosive materials respectively. The largest mass in case of Comp B and TNT for second value of thickness are $4.4572kg$ and $5.9168kg$ respectively. As these are largest mass values for thickness of $0.15m$, all fragments have mass smaller than $4.4572kg$ for Comp B and $5.9168kg$ for TNT.
Largest mass in case of RDX and Tetryl for thickness of $0.15m$, are $4.2656kg$ and $5.3292kg$ respectively. These being largest mass values, all fragments have mass smaller than $4.2656kg$ and $5.3292kg$ for RDX and Tetryl.

Tables (4.2 - 4.5) display the mass and densities (number) of fragments for different explosive types (Comp B, RDX, TNT and Tetryl) with shell thickness values $0.2m$ and $0.15m$. From tables 4.2 and 4.3 it can be observed that in case of Comp B and RDX explosive with $0.2m$ shell thickness, number of fragments with mass greater than $2kg$ account only about 18.52% and 16.94% of the total fragments. In case of shell thickness $0.15m$, the number of fragments with mass greater than $2kg$ account only about 3.23% and 2.98% of the total fragments. Similarly in case of TNT and

Table 4.2: Mass Distribution Interval in 2-D Fragmentation (Comp B Exp.)

| $thickness = 0.2m$ | | | $thickness = 0.15m$ | | |
|---|---|---|---|---|---|
| *Mass* | *Numbers* | *Percentage* | *Mass* | *Numbers* | *Percentage* |
| 9.01–10 | 0 | 0.00 | 9.01–10 | 0 | 0.00 |
| 8.01–9 | 0 | 0.00 | 8.01–9 | 0 | 0.00 |
| 7.01–8 | 0 | 0.00 | 7.01–8 | 0 | 0.00 |
| 6.01–7 | 0 | 0.00 | 6.01–7 | 0 | 0.00 |
| 5.01–6 | 1 | 0.93 | 5.01–6 | 0 | 0.00 |
| 4.01–5 | 2 | 1.85 | 4.01–5 | 0 | 0.00 |
| 3.01–4 | 6 | 5.65 | 3.01–4 | 1 | 0.46 |
| 2.01–3 | 11 | 10.19 | 2.01–3 | 6 | 2.76 |
| 1.01–2 | 27 | 25.00 | 1.01–2 | 33 | 15.21 |
| 0.0031–1 | 61 | 56.48 | 0.0031–1 | 177 | 81.57 |
| **Total** | 108 | | **Total** | 217 | |

Table 4.3: Mass Distribution Interval in 2-D Fragmentation (RDX Exp.)

| $thickness = 0.2m$ | | | $thickness = 0.15m$ | | |
|---|---|---|---|---|---|
| *Mass* | *Numbers* | *Percentage* | *Mass* | *Numbers* | *Percentage* |
| 9.01–10 | 0 | 0.00 | 9.01–10 | 0 | 0.00 |
| 8.01–9 | 0 | 0.00 | 8.01–9 | 0 | 0.00 |
| 7.01–8 | 0 | 0.00 | 7.01–8 | 0 | 0.00 |
| 6.01–7 | 0 | 0.00 | 6.01–7 | 0 | 0.00 |
| 5.01–6 | 1 | 0.85 | 5.01–6 | 0 | 0.00 |
| 4.01–5 | 2 | 1.69 | 4.01–5 | 0 | 0.00 |
| 3.01–4 | 5 | 4.24 | 3.01–4 | 1 | 0.42 |
| 2.01–3 | 12 | 10.17 | 2.01–3 | 6 | 2.51 |
| 1.01–2 | 29 | 24.58 | 1.01–2 | 34 | 14.23 |
| 0.0031–1 | 69 | 58.47 | 0.0031–1 | 198 | 82.85 |
| **Total** | 118 | | **Total** | 239 | |

Table 4.4: Mass Distribution Interval in 2-D Fragmentation (TNT Exp.)

| $thickness = 0.2m$ | | | $thickness = 0.15m$ | | |
|---|---|---|---|---|---|
| $Mass$ | $Numbers$ | $Percentage$ | $Mass$ | $Numbers$ | $Percentage$ |
| 9.01–10 | 0 | 0.00 | 9.01–10 | 0 | 0.00 |
| 8.01–9 | 0 | 0.00 | 8.01–9 | 0 | 0.00 |
| 7.01–8 | 1 | 1.85 | 7.01–8 | 0 | 0.00 |
| 6.01–7 | 1 | 1.85 | 6.01–7 | 0 | 0.00 |
| 5.01–6 | 1 | 1.85 | 5.01–6 | 0 | 0.00 |
| 4.01–5 | 3 | 5.56 | 4.01–5 | 0 | 0.00 |
| 3.01–4 | 4 | 7.41 | 3.01–4 | 3 | 2.73 |
| 2.01–3 | 8 | 14.81 | 2.01–3 | 7 | 6.36 |
| 1.01–2 | 13 | 24.07 | 1.01–2 | 23 | 20.91 |
| 0.0031–1 | 23 | 49.59 | 0.0031–1 | 77 | 70.00 |
| **Total** | 54 | | **Total** | 110 | |

Table 4.5: Mass Distribution Interval in 2-D Fragmentation (Tetryl Exp.)

| $thickness = 0.2m$ | | | $thickness = 0.15m$ | | |
|---|---|---|---|---|---|
| $Mass$ | $Numbers$ | $Percentage$ | $Mass$ | $Numbers$ | $Percentage$ |
| 9.01–10 | 0 | 0.00 | 9.01–10 | 0 | 0.00 |
| 8.01–9 | 0 | 0.00 | 8.01–9 | 0 | 0.00 |
| 7.01–8 | 0 | 0.00 | 7.01–8 | 0 | 0.00 |
| 6.01–7 | 1 | 1.41 | 6.01–7 | 0 | 0.00 |
| 5.01–6 | 1 | 1.41 | 5.01–6 | 0 | 0.00 |
| 4.01–5 | 3 | 4.23 | 4.01–5 | 0 | 0.00 |
| 3.01–4 | 5 | 7.04 | 3.01–4 | 2 | 1.39 |
| 2.01–3 | 9 | 12.68 | 2.01–3 | 7 | 4.86 |
| 1.01–2 | 18 | 24.35 | 1.01–2 | 27 | 18.75 |
| 0.0031–1 | 35 | 49.30 | 0.0031–1 | 108 | 75.30 |
| **Total** | 71 | | **Total** | 144 | |

Tetryl type with $0.2m$ shell thickness (tables 4.4 and 4.5) fragments with mass greater than $2kg$ accounts only about 33.33% and 26.76% of the total fragments respectively. However for $0.15m$ shell thickness the number of fragments with mass greater than $2kg$ account only about 9.09% and 6.25% of the total fragments.

### 4.2.2 Initial Velocities of Fragments

The velocity of the fragments can be divided into two parts:

- The initial velocity
- The velocity as a function of distance from the fragmentation point

The initial velocity of the fragments of a cylindrical warhead depends upon the mass of explosive, casing mass and characteristics of the Exp and is determined from the Gurney equation.

- Fragment Initial Velocity due to RDX Explosive is $1987.6m/s$
- Fragment Initial Velocity due to TNT Explosive is $1656.1m/s$
- Fragment Initial Velocity due to comp B Explosive is $1884.3m/s$
- Fragment Initial Velocity due to Tetryl Explosive is $1697.5m/s$

## 4.3 Distance Travel by Fragments and Dispersion Map

In order to calculate risks related to fragmentation (lethality range) of explosive munitions, trajectories of different fragments are calculated. The influence of air drag and gravity force has been taken into account. The initial values of velocity components in X, Y, Z directions are calculated for different values of initial throwing angles $\theta$ and $\phi$. MATLAB's function ODE45 has been used to compute the coordinates of the fragment during flight.

During the trajectory calculation, all fragments are assumed to have same initial fragment height. The ground distribution of fragments is determined by terminating the

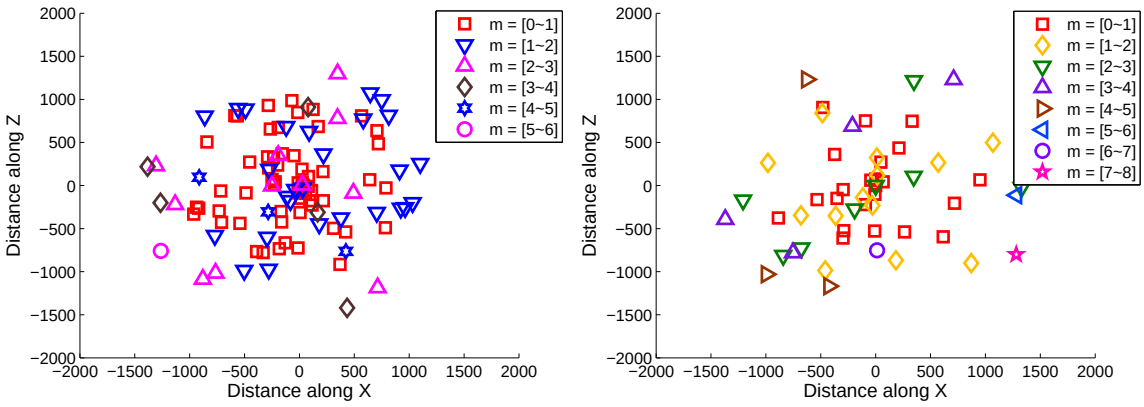


(a) Comp B (b) TNT

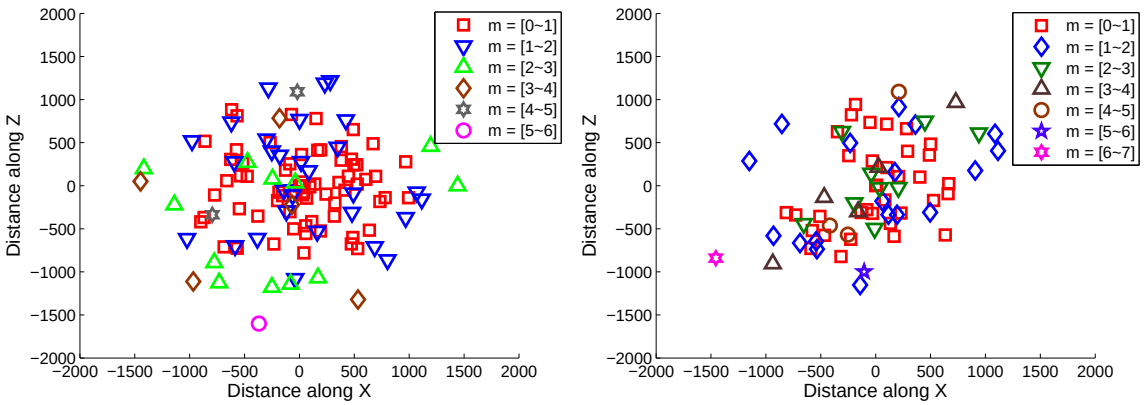


(c) RDX (d) Tetryl

Figure 4.3: Dispersion Map For Shell with Thickness of $0.2m$

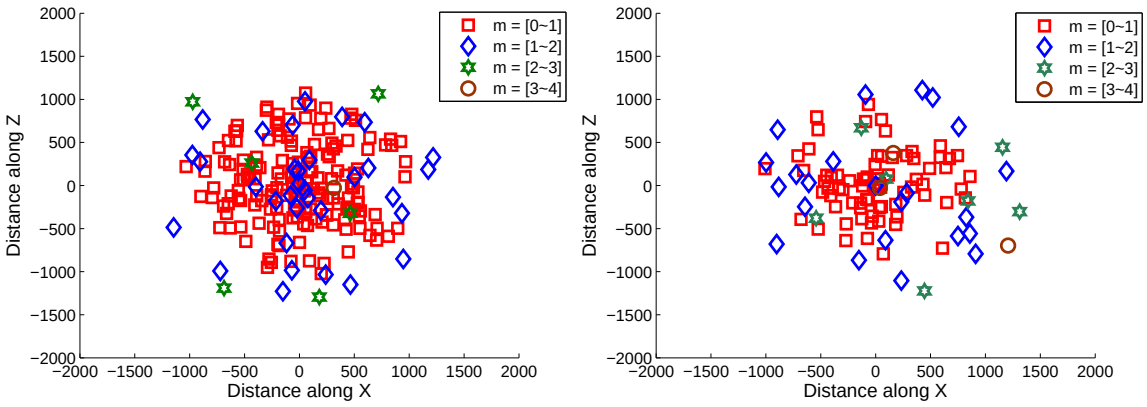


(a) Comp B




(b) TNT

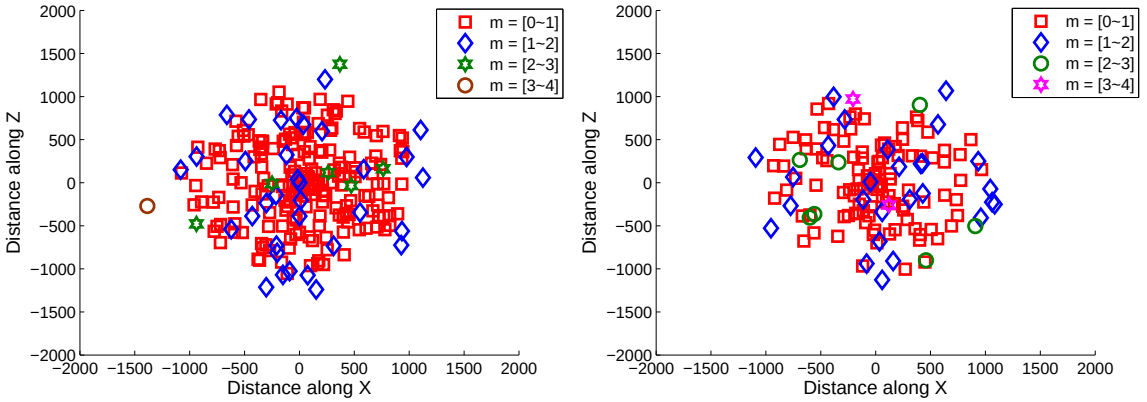


(c) RDX




(d) Tetryl

Figure 4.4: Dispersion Map For Shell with Thickness of $0.15m$

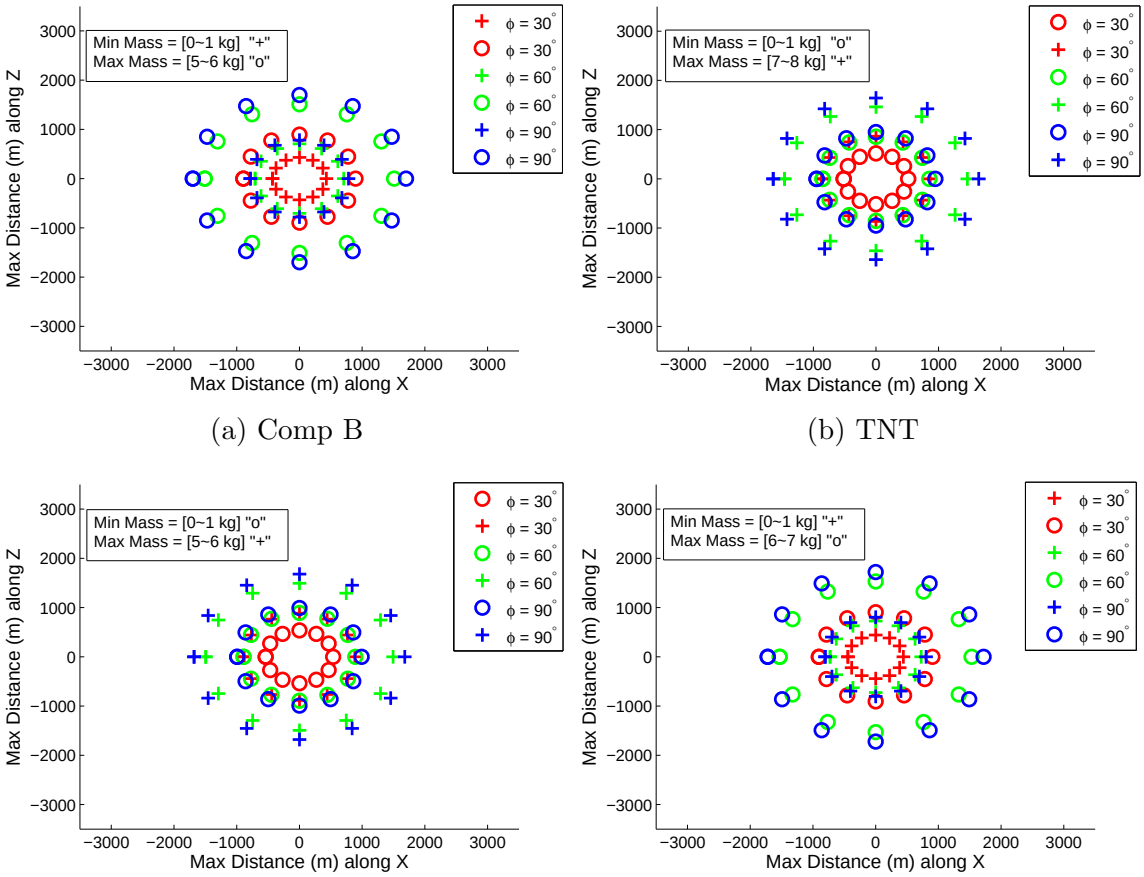


(a) Comp B

(b) TNT

(c) RDX

(d) Tetryl

Figure 4.5: Maximum Possible Dispersion Map For Shell with Thickness of $0.2m$

trajectory at the ground level (when $y = 0$).
Figures 4.3 - 4.4 show the dispersion of different fragments for each explosive types (Comp B, RDX, TNT and Tetryl) with shell thickness values ($0.2m$ and $0.15m$). The fragment mass and initial throwing angles are randomly sampled.

In order to estimate the maximum possible distance covered by fragments resulted from 2-D fragmentation of cylindrical shell, it was important to consider systematic variation in initial throwing angles $\theta$ ($0° : 30° : 360°$) and $\phi(0° : 30° : 90°)$. Figures 4.5 and 4.6 shows the maximum possible dispersion of a smallest and largest mass fragments for all four types of explosive material with a shell thickness of $0.2m$. It can be observed that light fragments travel much shorter distances and fall in higher density regions. In contrast, owing to stronger the speed storing ability and higher

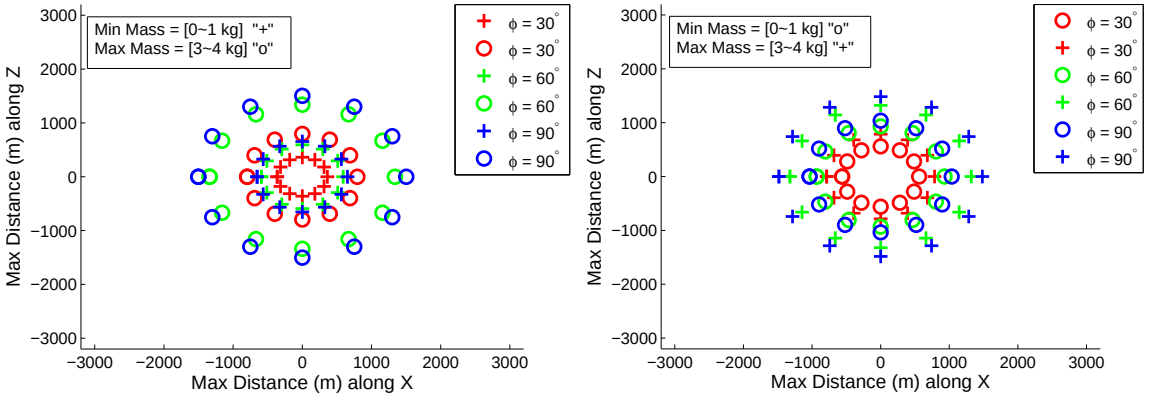


(a) Comp B




(b) TNT

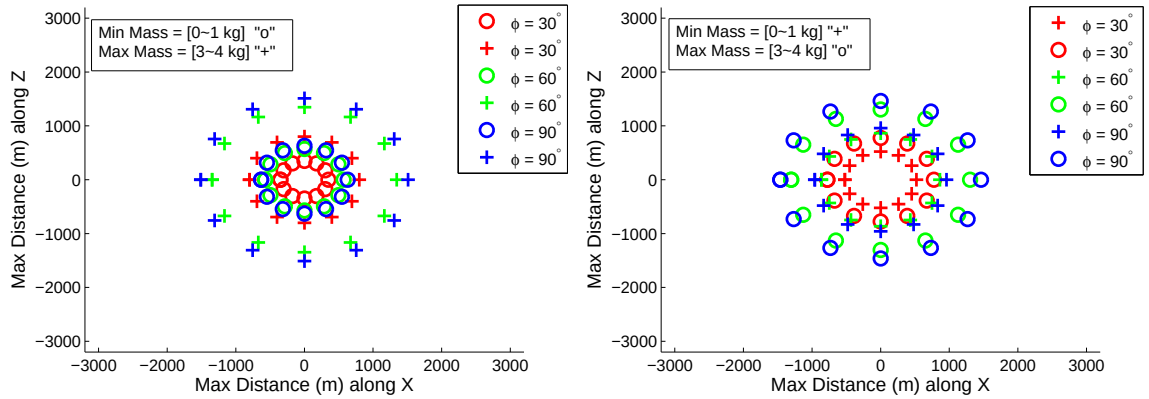


(c) RDX




(d) Tetryl

Figure 4.6: Maximum Possible Dispersion Map For Shell with Thickness of $0.15m$

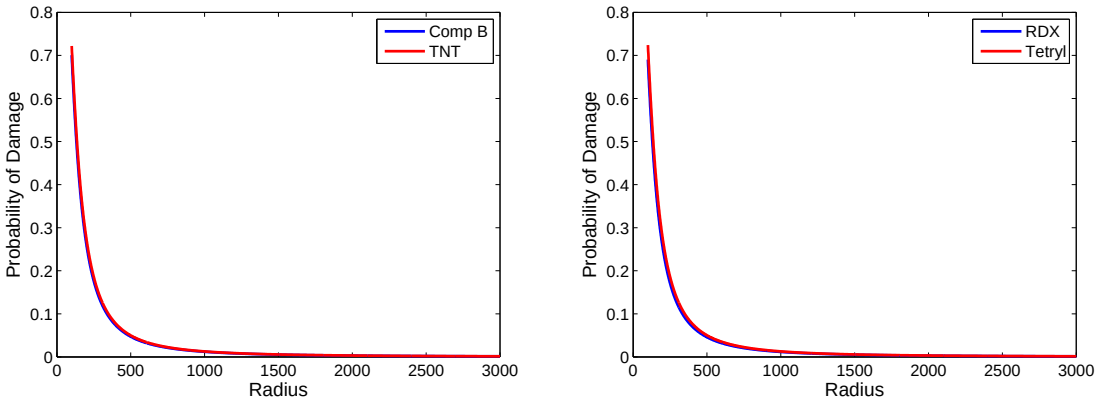


(a) Comp B and TNT

(b) RDX and Tetryl

Figure 4.7: Probability of Damage Based on Minimum Mass at Standing Position

kinetic energy of heavy fragments, they have traveled a long distance.
Maximum distance traveled by the largest mass fragments is around $1500m$ and $2000m$ in case of $0.2m$ and $0.15m$ shell thickness respectively.

## 4.4 Probability of Damage to Human at Different Position

The probability that a fragment would impact a particular target (human) has been predicted using the equations (3.12 and 3.13).

### 4.4.1 Person in Standing Position

Figure 4.7 (a)(b) show the probability of being hit by the minimum mass fragments, when a person is in standing position, facing the explosion and taking no evasive action. It can be observed that the probability of being hit is maximum at the origin and decreases with increasing distance from the point of explosion. The probability of damage is 0.7 at the origin (fragmentation point), 0.1 at a distance of $500m$ and almost zero at a distance of $1000m$.

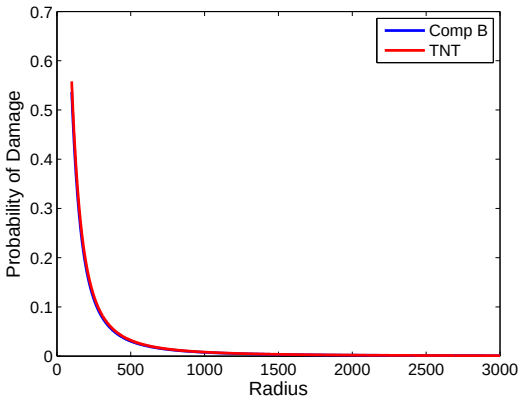


(a) Comp B and TNT

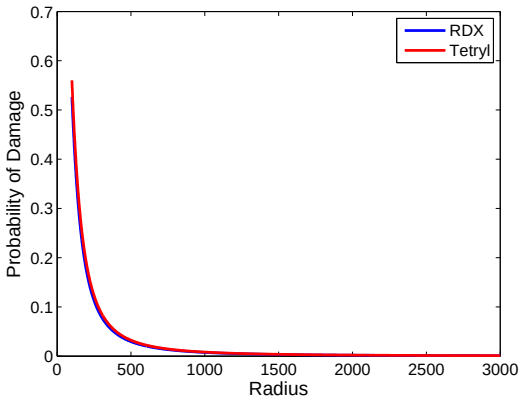


(b) RDX and Tetryl

Figure 4.8: Probability of Damage Based on Minimum Mass at Assault Position

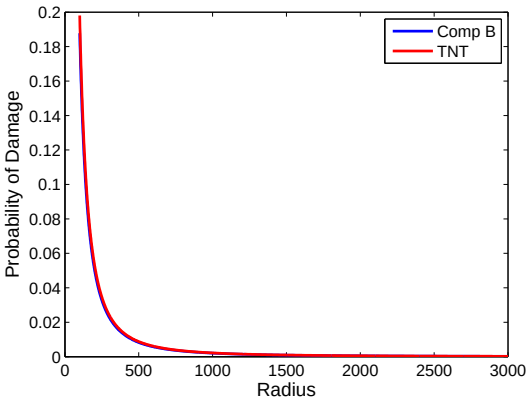


(a) Comp B and TNT

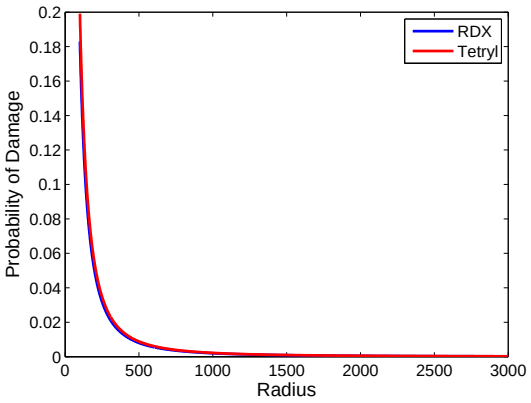


(b) RDX and Tetryl

Figure 4.9: Probability of Damage Based on Minimum Mass at Supine Position

### 4.4.2 Person in Assault Position

Figure 4.8 (c)(d) illustrate the probability of damage by the minimum mass fragments, when a human is in sitting position near the point of explosion. It is evident from the graph that, for assaulted position the probability from origin (fragmentation point) is 0.6 and it starts declining until it reaches a distance $500m$. At a distance of $500m$ probability is 0.1. After a distance of about $700m$, the probability is almost zero.

### 4.4.3 Person in Supine Position

Figure 4.9 (e)(f) demonstrations the probability of being hit by the minimum mass fragments, when a person is in supine position. For a supine position probability start with 0.2 from the fragmentation point. At a distance of $250m$ it reaches a value of 0.1. After a distance of $500m$ the probability is almost zero.

# Chapter 5

# 3-D Fragmentation of Cylindrical Shells

This chapter deals with the 3-D fragmentation of a cylindrical shell. The important parameters (fragment numbers, mass distribution of fragments and the initial velocity) required to estimate the risks of human injury due to 3-D fragmentation of a cylindrical shell, are calculated. The details of the study are given in following paragraphs.

## 5.1 Parameters of Explosive Munitions

The properties of explosive munitions used for the 3-D fragmentation analysis of cylindrical shells are shown in Table 4.1. A limited parametric study is performed to estimate the risks of human injury from fragments, considering

- Various explosive types
- Different shell thickness

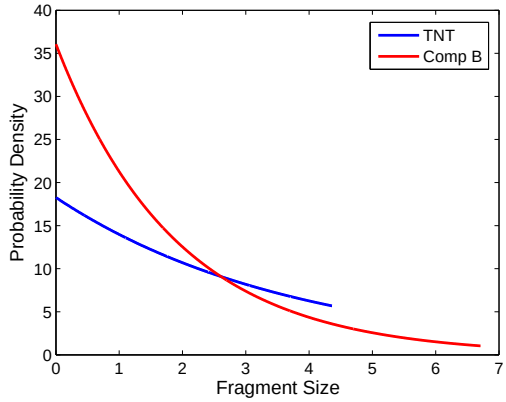


(a) Comp B,TNT

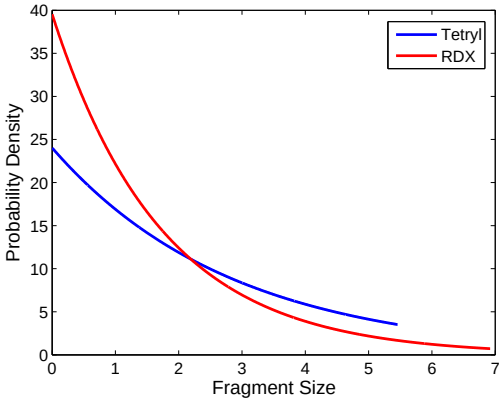


(b) RDX,Tetryl

Figure 5.1: Fragmentation Pattern for 3-D Mott Distribution with a Thickness of Shell $0.2m$

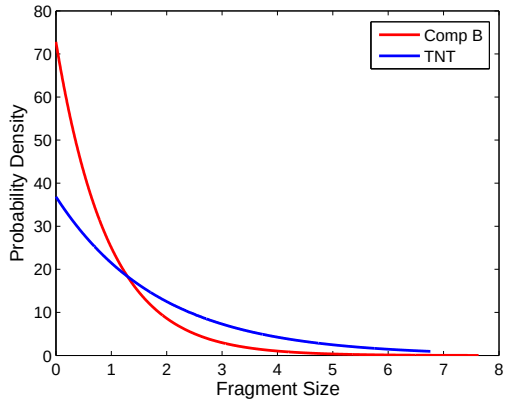


(a) Comp B,TNT

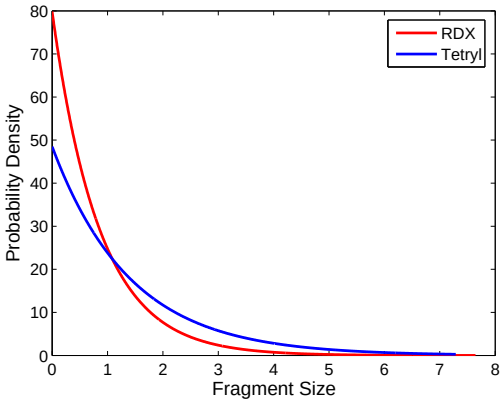


(b) RDX,Tetryl

Figure 5.2: Fragmentation Pattern for 3-D Mott Distribution with a Thickness of Shell $0.15m$

## 5.2 Fragments Characteristic Parameters

### 5.2.1 Number and Mass Distribution of Fragments

3-D fragmentation implies fractures through all three dimensions of a fragmenting body and produces the fragments with size $t^* < t$ (shell thickness). It is considered as the most important and most complex case of fragmentation from the application point of view. The Mott formula (equations 3.1 and 3.2) are used for estimation of fragments number and mass distribution.

Figure 5.1 shows the fragmentation pattern based on 3-D Mott Distribution by considering four different types of explosives (Comp B, TNT, RDX and Tetryl) with a shell thickness of $0.2m$. The total number of fragments generated are estimated to be 36, 18, 40 and 24 for Comp B, TNT, RDX and Tetryl explosive respectively. The masses of the largest fragment in case of Comp B and TNT are $6.7085kg$ and $4.3624kg$ respectively. As these are largest mass values, all fragments have mass smaller than $6.7085kg$ for Comp B and $4.3624kg$ in case of TNT explosive. On the other hand largest mass in case of RDX and Tetryl for shell thickness of $0.2m$, are $6.9196kg$ and $5.4573kg$ respectively.

Figure 5.2 shows the fragment mass distribution in 3-D fragmentation of the cylindrical shell with Comp B, TNT, RDX and Tetryl type explosive for thickness of $0.15m$. The total number of fragments generated, are estimated to be 73, 37, 80 and 49 for Comp B, TNT, RDX and Tetryl explosive materials respectively. The largest mass in case of Comp B and TNT for second value of thickness are $7.6328kg$ and $6.7608kg$ respectively. Similarly, the largest mass in the case of RDX and Tetryl, are $7.6454kg$ and $7.2880kg$ respectively.

Tables (5.1 - 5.4) display the mass and densities (number) of fragments for different explosive types (Comp B, RDX, TNT and Tetryl) with shell thickness values $0.2m$ and $0.15m$. From tables 5.1 and 5.2 it can be observed that in case of Comp B and RDX explosive with $0.2m$ shell thickness, number of fragments with mass greater than $2kg$ account only about 33.33% and 30.76% of the total fragments. In case of shell thickness $0.15m$, the number of fragments with mass greater than $2kg$ account only about 11.11% and 8.86% of the total fragments. Similarly in case of TNT and Tetryl type with $0.2m$ shell thickness (tables 5.3 and 5.4) fragments with mass greater than $2kg$ accounts only about 60% and 54.16% of the total fragments respectively. However for $0.15m$ shell thickness the number of fragments with mass greater than

Table 5.1: Mass Distribution Interval in 3-D Fragmentation (Comp B Exp.)

| $thickness = 0.2m$ | | | $thickness = 0.15m$ | | |
|---|---|---|---|---|---|
| *Mass* | *Numbers* | *Percentage* | *Mass* | *Numbers* | *Percentage* |
| 9.01–10 | 0 | 0.00 | 9.01–10 | 0 | 0.00 |
| 8.01–9 | 0 | 0.00 | 8.01–9 | 0 | 0.00 |
| 7.01–8 | 0 | 0.00 | 7.01–8 | 0 | 0.00 |
| 6.01–7 | 1 | 2.78 | 6.01–7 | 0 | 0.00 |
| 5.01–6 | 1 | 2.78 | 5.01–6 | 0 | 0.00 |
| 4.01–5 | 2 | 5.56 | 4.01–5 | 0 | 0.00 |
| 3.01–4 | 3 | 8.33 | 3.01–4 | 2 | 2.78 |
| 2.01–3 | 5 | 13.89 | 2.01–3 | 6 | 8.33 |
| 1.01–2 | 9 | 25.00 | 1.01–2 | 16 | 22.22 |
| 0.0031–1 | 15 | 41.67 | 0.0031–1 | 48 | 66.67 |
| **Total** | 36 | | **Total** | 72 | |

Table 5.2: Mass Distribution Interval in 3-D Fragmentation (RDX Exp.)

| $thickness = 0.2m$ | | | $thickness = 0.15m$ | | |
|---|---|---|---|---|---|
| *Mass* | *Numbers* | *Percentage* | *Mass* | *Numbers* | *Percentage* |
| 9.01–10 | 0 | 0.00 | 9.01–10 | 0 | 0.00 |
| 8.01–9 | 0 | 0.00 | 8.01–9 | 0 | 0.00 |
| 7.01–8 | 0 | 0.00 | 7.01–8 | 0 | 0.00 |
| 6.01–7 | 1 | 2.56 | 6.01–7 | 0 | 0.00 |
| 5.01–6 | 1 | 2.56 | 5.01–6 | 0 | 0.00 |
| 4.01–5 | 1 | 2.56 | 4.01–5 | 0 | 0.00 |
| 3.01–4 | 3 | 7.69 | 3.01–4 | 2 | 2.53 |
| 2.01–3 | 6 | 15.38 | 2.01–3 | 5 | 6.33 |
| 1.01–2 | 10 | 25.64 | 1.01–2 | 17 | 21.52 |
| 0.0031–1 | 17 | 43.59 | 0.0031–1 | 55 | 69.62 |
| **Total** | 39 | | **Total** | 79 | |

Table 5.3: Mass Distribution Interval in 3-D Fragmentation (TNT Exp.)

| $thickness = 0.2m$ | | | $thickness = 0.15m$ | | |
|---|---|---|---|---|---|
| $Mass$ | $Numbers$ | $Percentage$ | $Mass$ | $Numbers$ | $Percentage$ |
| 9.01–10 | 0 | 0.00 | 9.01–10 | 0 | 0.00 |
| 8.01–9 | 1 | 6.67 | 8.01–9 | 0 | 0.00 |
| 7.01–8 | 1 | 6.67 | 7.01–8 | 0 | 0.00 |
| 6.01–7 | 1 | 6.67 | 6.01–7 | 1 | 2.78 |
| 5.01–6 | 1 | 6.67 | 5.01–6 | 1 | 2.78 |
| 4.01–5 | 1 | 6.67 | 4.01–5 | 2 | 5.36 |
| 3.01–4 | 2 | 13.33 | 3.01–4 | 3 | 8.33 |
| 2.01–3 | 2 | 13.33 | 2.01–3 | 5 | 13.89 |
| 1.01–2 | 2 | 13.33 | 1.01–2 | 9 | 25.00 |
| 0.0031–1 | 4 | 26.67 | 0.0031–1 | 15 | 41.08 |
| **Total** | 15 | | **Total** | 36 | |

Table 5.4: Mass Distribution Interval in 3-D Fragmentation (Tetryl Exp.)

| $thickness = 0.2m$ | | | $thickness = 0.15m$ | | |
|---|---|---|---|---|---|
| $Mass$ | $Numbers$ | $Percentage$ | $Mass$ | $Numbers$ | $Percentage$ |
| 9.01–10 | 1 | 4.17 | 9.01–10 | 0 | 0.00 |
| 8.01–9 | 1 | 4.17 | 8.01–9 | 0 | 0.00 |
| 7.01–8 | 1 | 4.17 | 7.01–8 | 0 | 0.00 |
| 6.01–7 | 1 | 4.17 | 6.01–7 | 0 | 0.00 |
| 5.01–6 | 1 | 4.17 | 5.01–6 | 1 | 2.08 |
| 4.01–5 | 2 | 8.33 | 4.01–5 | 1 | 2.08 |
| 3.01–4 | 2 | 8.33 | 3.01–4 | 3 | 6.25 |
| 2.01–3 | 4 | 16.67 | 2.01–3 | 6 | 12.50 |
| 1.01–2 | 4 | 16.67 | 1.01–2 | 12 | 25.00 |
| 0.0031–1 | 7 | 29.17 | 0.0031–1 | 25 | 52.08 |
| **Total** | 24 | | **Total** | 48 | |

$2kg$ account only about 33.33% and 22.917% of the total fragments.

### 5.2.2 Initial Velocities of Fragments

The initial velocity of the fragments generated from the 3-D fragmentation of a cylindrical warhead is determined from the Gurney equation (3.3 and 3.4).

- Fragment Initial Velocity due to RDX Explosive is $1987.6m/s$
- Fragment Initial Velocity due to TNT Explosive is $1656.1m/s$
- Fragment Initial Velocity due to comp B Explosive is $1884.3m/s$
- Fragment Initial Velocity due to Tetryl Explosive is $1697.5m/s$

## 5.3 Distance Travel by Fragments and Dispersion Map

In order to calculate risks (lethality range) associated with the 3-D fragmentation of cylindrical explosive munitions, trajectories of different fragment are calculated. The influence of air drag and gravity force has been taken into account. The initial values of velocity components in X, Y, Z directions, are calculated for different values of initial throwing angles $\theta$, and $\phi$. MATLAB's function ODE45 has been used to compute the coordinates of the fragments during flight.
During the trajectory calculation, all fragments are assumed to have same initial fragment height. The ground distribution of fragments is determined by terminating the trajectory at the ground level ($y = 0$).

Figures (5.3 - 5.4) show the dispersion of different fragments of four different explosive types (Comp B, RDX, TNT and Tetryl) with shell thickness values ($0.2m$ and $0.15m$). The fragment mass and initial throwing angles are randomly sampled.
For the estimation of the maximum possible damage area of fragments generated in 3-D fragmentation of cylindrical shell, it was important to consider systematic variation in initial throwing angles $\theta(0^\circ : 30^\circ : 360^\circ)$ and $\phi(0^\circ : 30^\circ : 90^\circ)$. Figures 5.5 and 5.6 show the maximum possible dispersion of a smallest and largest mass fragments

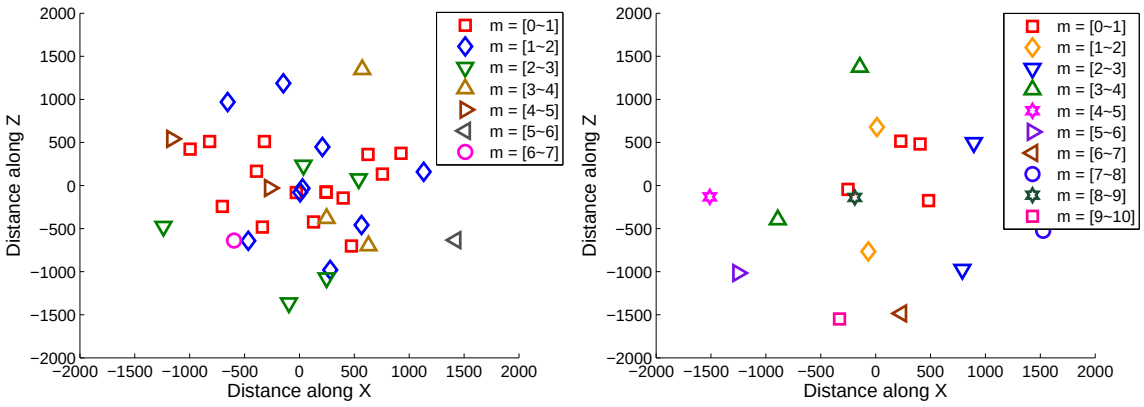


(a) Comp B




(b) TNT

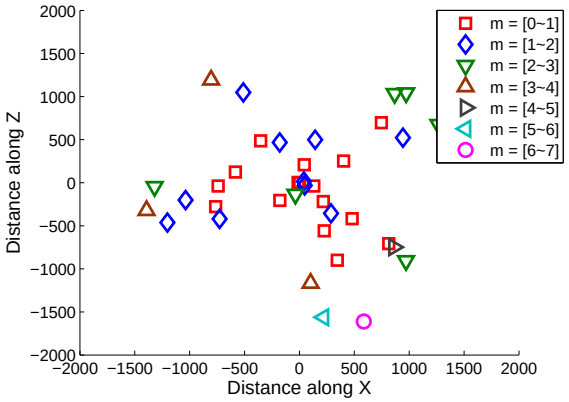


(c) RDX

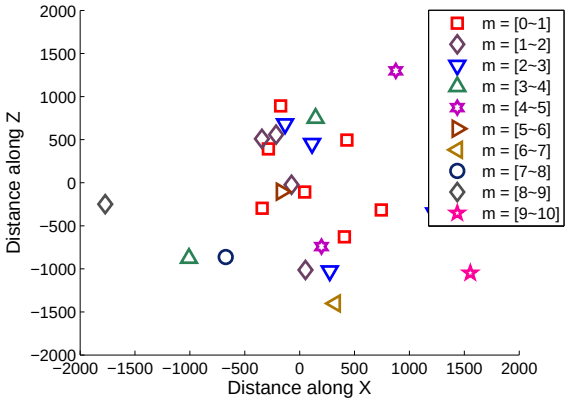


(d) Tetryl

Figure 5.3: Dispersion Map For Shell with Thickness of $0.2m$

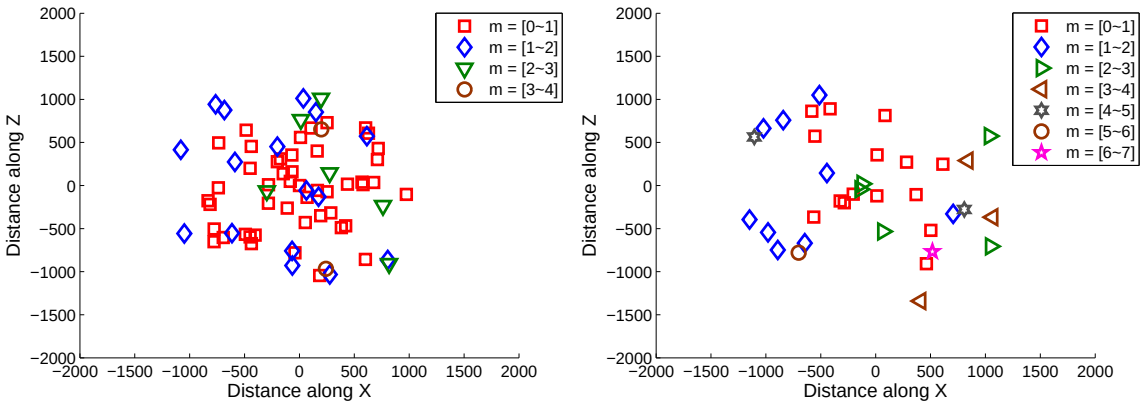


(a) Comp B




(b) TNT

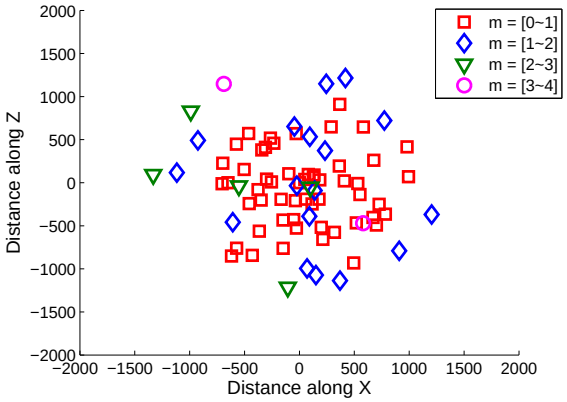


(c) RDX

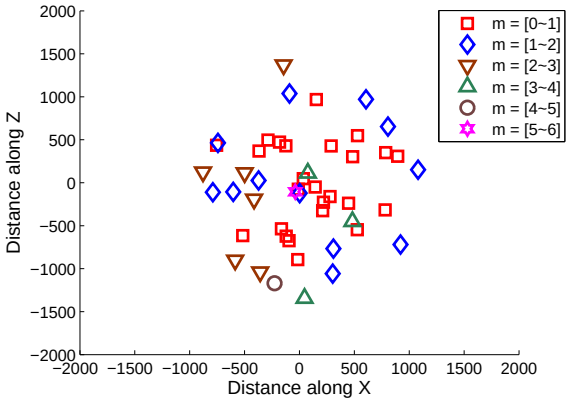


(d) Tetryl

Figure 5.4: Dispersion Map For Shell with Thickness of $0.15m$

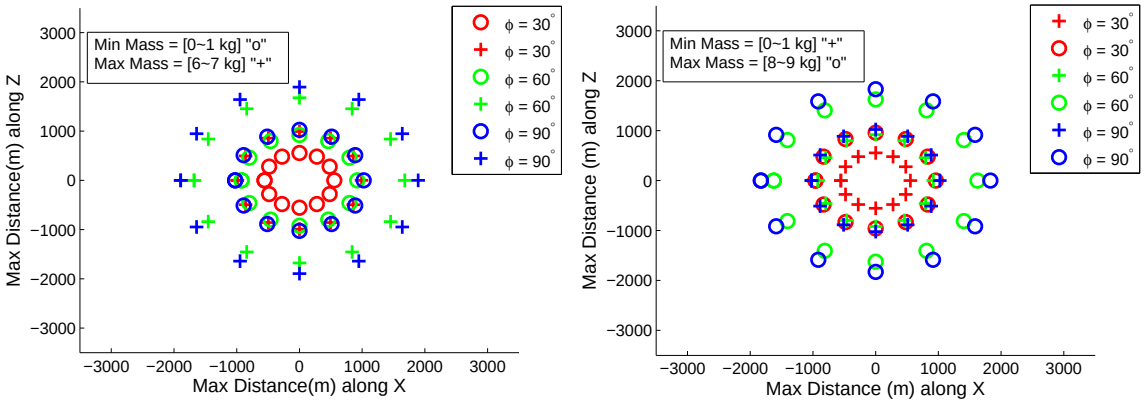


(a) Comp B




(b) TNT

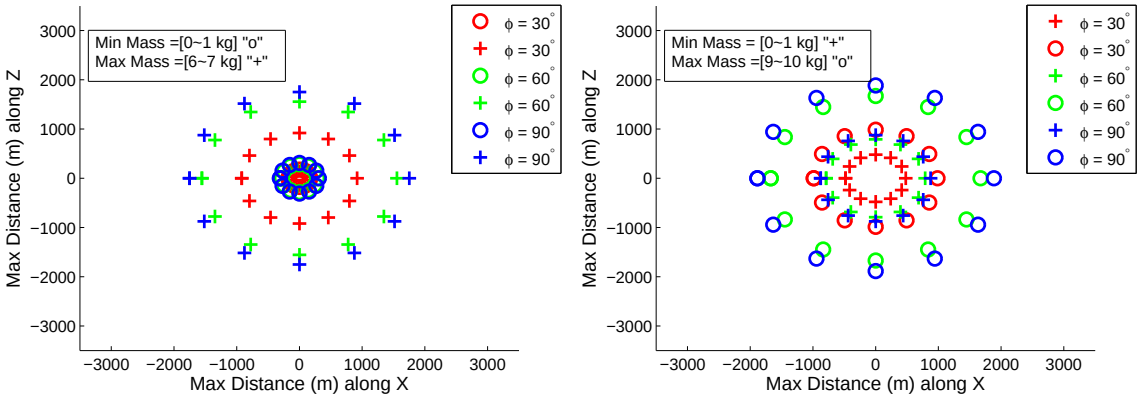


(c) RDX




(d) Tetryl

Figure 5.5: Maximum Possible Dispersion Map For Shell with Thickness of $0.2m$

for all four types of explosive material with different shell thickness values ($0.2m$ and $0.15m$). It can be observed that light fragments travel much shorter distances and fall in higher density regions. In contrast, owing to stronger the speed storing ability and higher kinetic energy of heavy fragments, they have traveled a long distance. Moreover, in case of large-mass fragments, the impact velocity arriving at the target point is also expected to be higher.

It can be observed from these figures (5.5 - 5.6) that light fragments travel much shorter distances and fall in higher density regions. In contrast, the heavy fragments travel a long distance.

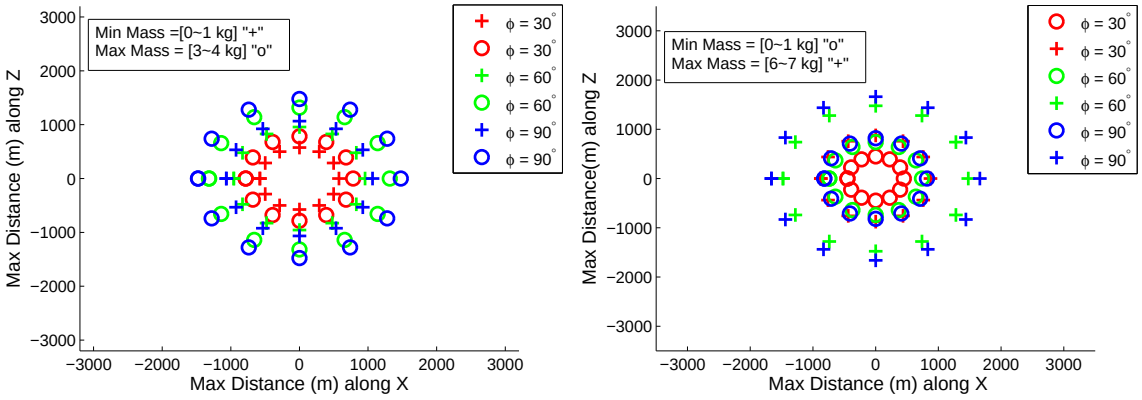


(a) Comp B




(b) TNT

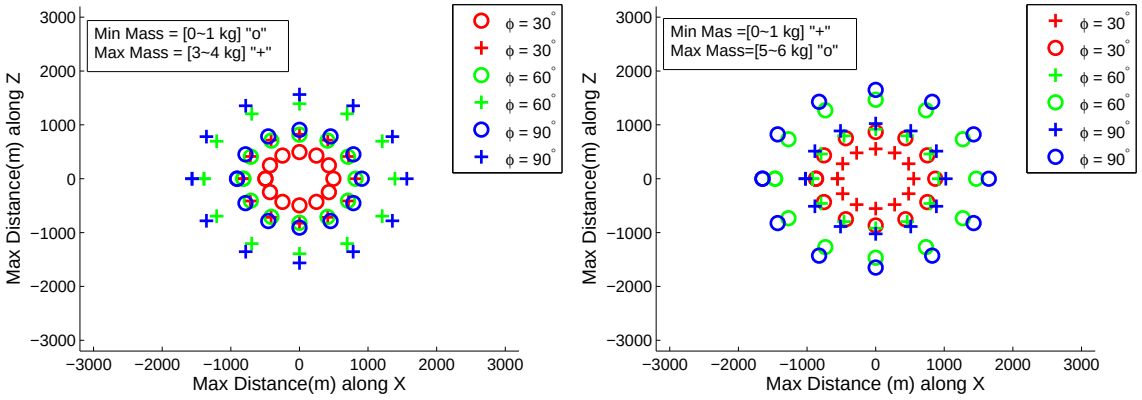


(c) RDX




(d) Tetryl

Figure 5.6: Maximum Possible Dispersion Map For Shell with Thickness of $0.15m$

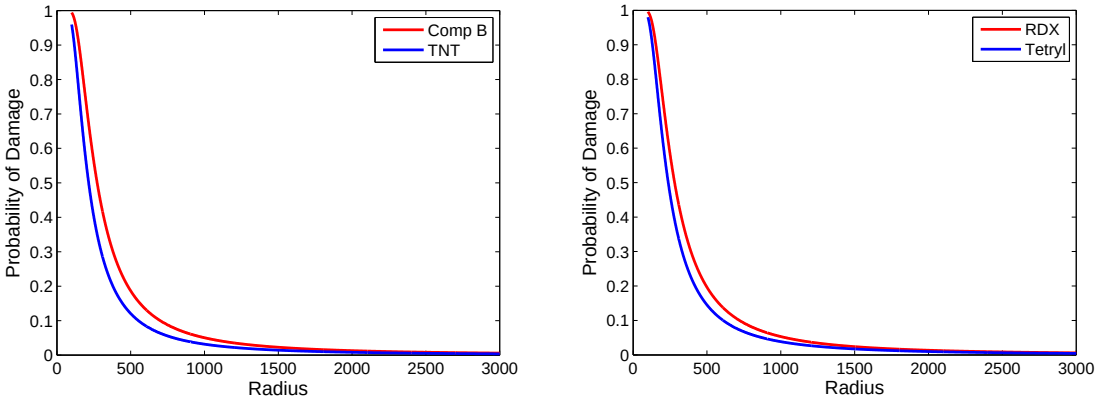


(a) Comp B and TNT

(b) RDX and Tetryl

Figure 5.7: Probability of Damage Based on Minimum Mass at Standing position

## 5.4 Probability of Damage For Human at Different Position

The probability that a fragment would impact a particular target (human) has been predicted using the equations (3.12 - 3.13).

### 5.4.1 Person in Standing Position

Figure 5.7 (a)(b) show the probability of being hit by the minimum mass fragments, when a person is in standing position, facing the explosion and taking no evasive action. It can be observed that the probability of being hit is maximum at the origin and decreases with increasing distance from the point of explosion. The probability of the minimum mass fragment to hit a human target is 100% at the origin (fragmentation point), 10% at $1000m$ distance from the origin and negligible afterwards

### 5.4.2 Person in Assault Position

Figure 5.8 (c)(d) illustrate the probability of damage by the minimum mass fragments when a human is in sitting position near the point of explosion. It is evident from

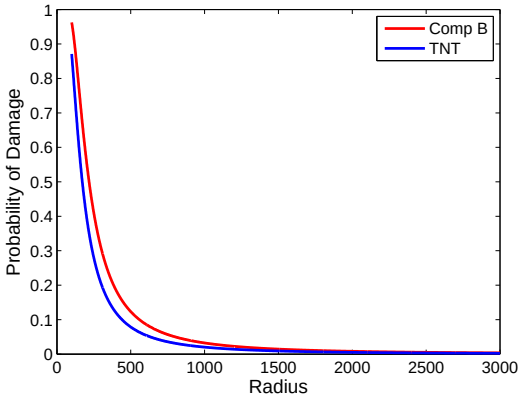


(a) Comp B and TNT

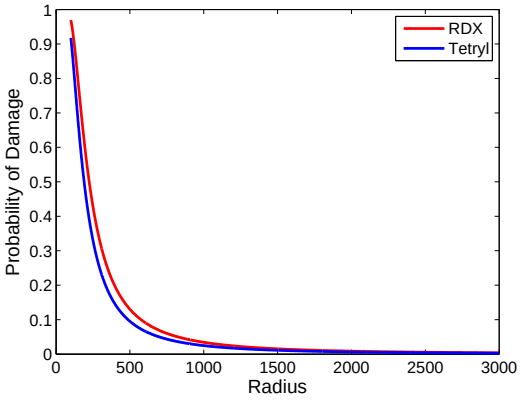


(b) RDX and Tetryl

Figure 5.8: Probability of Damage Based on Minimum Mass at Assaulted position

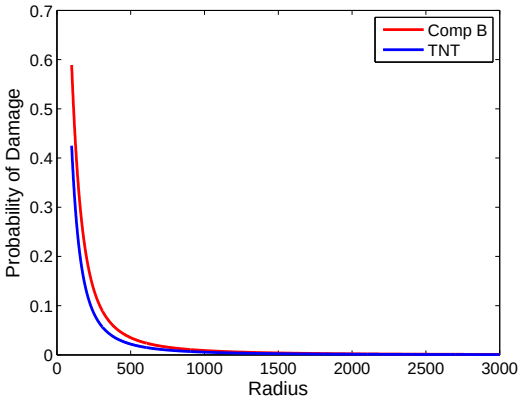


(a) Comp B and TNT

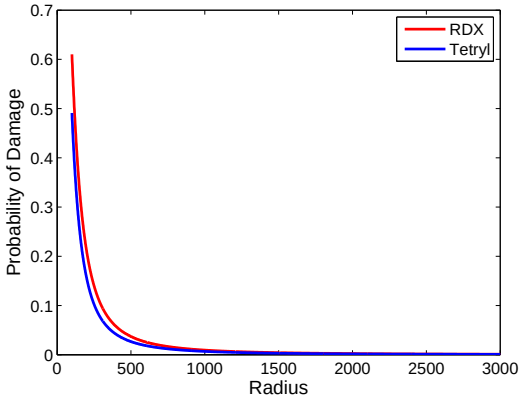


(b) RDX and Tetryl

Figure 5.9: Probability of Damage Based on Minimum Mass at Supine position

the graph that, the probability of being hit is maximum near the point of explosion and then starts to decline until it reaches a distance $700m$. Beyond $700m$ range, we neglect the probability value and considered as zero.

### 5.4.3 Person in Supine Position

Figure 5.9 (e)(f) demonstrates the probability of being hit by the maximum, when a person is in supine position. For comp B, TNT, the probability of damage is 0.6 and 0.4 near the origin and 0.1 at $250m$ distance from origin. While for RDX and Tetryl probability start with $0.6, 0.5$ values, respectively until it reaches a distance of $250m$ where the probability is around 0.1.

# Chapter 6

# Conclusion and Recommendations

The key objective of this research is to estimate the terminal impact of fragments produced in 2-D and 3-D fragmentation of cylindrical explosive munitions. Mott formulation is used for estimation of fragment mass distribution in 2D and 3D cases. Fragment trajectories under the action of constant drag and Gravity are calculated from three dimensional equations of motion. A limited parametric study is performed to estimate the risks of human injury from 2D and 3D fragmentation of cylindrical explosive munitions, by considering.

- Various Explosive Types
- Different Shell Thickness. .

The significant conclusions of this work are summarized as follows.

- Both in 2-D and 3-D fragmentation cases
  - Light fragments are produced in large numbers.
  - Fragment mass distribution is different for different explosive types and shell thickness values.
  - Light fragments travel much shorter distances and fall in higher density regions. In contrast, owing to stronger the speed storing ability and higher kinetic energy of heavy fragments, they have traveled a long distance.
  - Maximum distance covered by a fragment is around $2000m$.
- In case of 2-D fragmentation
  - The probability of being hit by the minimum mass fragments, when a person is in standing position is around 70% between 0 and $250m$ distance, around 10% at a $500m$ distance and almost zero at a distance of $1000m$.

  - The probability of being hit by the minimum mass fragments, when a person is in assault position is around 50% between 0 and 250$m$ distance, around 10% at a 500$m$ distance and almost zero at a distance of 1000$m$.
  - The probability of being hit by the minimum mass fragments, when a person is in the supine position is around 20% between 0 and 250$m$ distance, below 10% at a 500$m$ distance and almost zero afterwards.

- In case of 3-D fragmentation

  - The probability of being hit by the minimum mass fragments, when a person is in standing position is 100% between 0 and 250$m$ distance, around 20% at a 500$m$ distance and almost 10% at a distance of 1000$m$.
  - The probability of being hit by the minimum mass fragments, when a person is in assault position is around 90% between 0 and 250$m$ distance, around 10% at a 500$m$ distance and almost zero at a distance of 1000$m$.
  - The probability of being hit by the minimum mass fragments, when a person is in the supine position is between 40 to 60% between 0 and 250$m$ distance, around 20% at a 500$m$ distance and almost zero afterwards.

The recommendation for future work are given in below.

- Influence of geometrical shapes of fragments should be included in the study.
- The effect of warhead design on natural fragmentation performances should be investigated.
- With recent advancements in computational resource, numerical Simulation techniques can also be used to study fragmentation process in high explosive projectiles .

# Bibliography


[1] Gudowska-Nowak, E., et al.,Distribution of DNA fragment sizes after irradiation with ions. *The European Physical Journal, vol. 30, pp 317-324, 2009*

[2] Holian, Brad Lee, and Dennis E. Grady.,Fragmentation by molecular dynamics: The microscopic "big bang". *Physical Review Letters, vol. 60, pp 1355-1358, 1988*

[3] Singh, P. K., et al., Rock fragmentation control in opencast blasting. *Journal of Rock Mechanics and Geotechnical Engineering, vol. 8.2, pp 225-237, 2016*

[4] Stephen A. Nelson *Meteorites,Impact and Mass Extraction* Natural Disasters, Tulane University, 2014

[5] Dittberner, Gerald, Jeff Elder, and Duncan Steel.,Orbital debris damage estimates using coupled pre-and post-impact calculations. *29th Aerospace Sciences Meeting 1991*

[6] How are Supernova formed and are there any getting ready to form now *https://spaceplace.nasa.gov/review/dr-marc-space/supernovas.html*, 2016

[7] Akhavan, Jacqueline. *The chemistry of explosives.* Royal Society of Chemistry, 2011

[8] Stacey, Weston M., *Nuclear reactor physics* . John Wiley & Sons, 2007

[9] Ngo, T., et al.,Blast loading and blast effects on structures–an overview. *Electronic Journal of Structural Engineering, vol. 7, pp 76-91, 2007*

[10] Glasstone, Samuel.,The effects of Nuclear Weapons *3rd Ed., U.S Depart of Defense and U.S Depart of Energy, Government Printing Office, Washington DC, 1977*

[11] Zehrt Jr, Willam H., and Michelle M. Crull., Development of Primary Fragmentation Separation Distances for Cased Cylindrical Munitions *Army Engineering and Support Center Huntsville, 1998*

[12] Klein, P.F.,Fragments and Hazards *Departments of Defense Explosives Safety Board, Washington, D.C, 1975*

[13] Pape, Ronald, Kim R. Mniszewski, and Anatol Longinow.,Explosion phenomena and effects of explosions on structures. II: Methods of analysis (explosion effects). *Practice Periodical on Structure Design and Constructions, vol. 15.2, pp 141-152, 2009*

[14] Medard, Louis A., Accidential Explosions; Physical and Chemical Properties. *vol 1, 1989*

[15] Covey, Dana C., and Christopher T. Born.,Blast injuries: mechanics and wounding patterns. *Journal of surgical orthopaedic advances, vol. 19.1, pp 8, 2010*

[16] DePalma, Ralph G., et al.,Blast injuries. *New England Journal of Medicine, vol. 352.13, 2005*

[17] Rosin, Paul.,The laws governing the fineness of powdered coal *Journal of Institute of Fuel, vol. 7, pp 29-36, 1933*

[18] Schuhmann, E.V.,Principles of communication, size distribution and surface calculations. *AIME Technical Publication, vol. 1189, pp 1-11, 1941*

[19] Macıas-Garcıa, A., Eduardo M. Cuerda-Correa, and M. A. Dıaz-Dıez.,Application of the Rosin–Rammler and Gates–Gaudin–Schuhmann models to the particle size distribution analysis of agglomerated cork. *Material Characterization, vol. 52, pp 159-164, 2004*

[20] Loveland, Peter J., and W. Richard Whalley.,Particle size analysis. *Smith Ka; Mullins Ce Soil analysis–physical methods, pp 281-314, 1992*

[21] Wu, S. Z., K. T. Chau, and T. X. Yu.,Crushing and fragmentation of brittle sphere under double Impact test. *Powder Technology, vol. 143, pp 41-55, 2004*

[22] Ouchiyama, N., S. L. Rough, and J. Bridgwater.,A population balance approach to describing bulk attrition. *Chemical engineering science, vol. 60, pp 1429-1440, 2005*

[23] Mott, N. F. and Linfoot, E.H.,A theory of fragmentation. *United Kingdom Ministry of Supply AC3348, February 1943*

[24] Mott, N. F.,Fragmentation of shell casings and the theory of rupture in metals. *Proceeding of Royal Society of London Series A-Mathematical and Physical Sciences, vol. 189, pp 300-308, 1947*

[25] Lienau, C. C.,Random Fracture for brittle solid *Journal of Franklin Institute, vol. 221, pp 485-494, 1936*

[26] Grady, D. E., and M. E. Kipp.,Geometric statistics and dynamic fragmentation. *Journal of Applied Physics, vol. 58, no 33, pp 1210-1222, 1985*

[27] Coles, Peter.,Voronoi cosmology. *Nature, vol. 349, pp 461-472, 1991*

[28] Ringler, Todd, Lili Ju, and Max Gunzburger.,A multiresolution method for climate system modeling: application of spherical centroidal Voronoi tessellations. *Ocean Dynamics, vol. 58.5, pp 475-498, 2008*

[29] Aurenhammer, Franz, Voronoi diagrams- A survey of fundamental geometric data structure. *ACM Computing Surveys(CSUR), vol. 23.3, pp 345-405, 1991*

[30] Manzini, Gianmarco, Alessandro Russo, and N. Sukumar.,New perspectives on polygonal and polyhedral finite element methods. *Computational Mechanics, vol. 44.4, pp 455-471, 2009*

[31] Kiang, T.,Mass distributions of asteroids, stars and galaxies. *Zeitschrift fur Astrophysik, vol. 64, pp 426-432, 1966*

[32] Grady, D. E., and M. E. Kipp.,Experimental measurement of dynamic failure and fragmentation properties of metals. *International Journal of solids and structures, vol. 32 , pp 2779-2791, 1995*

[33] Grady, D. E., et al.,Comparing alternate approaches in the scaling of naturally fragmenting munitions. *Proceeding of the 19th International Symposium on Ballistics, Interlaken, Switzerland, pp 591-597, 2001*

[34] Grady, Dennis E, Comparison of hypervelocity fragmentation and spall experiments with Tuler–Butcher spall and fragment size criteria. *International journal of impact engineering, vol. 33.1, pp 305-315, 2006*

[35] Strømsøe, E., and K. O. Ingebrigtsen, A modification of the Mott formula for prediction of the fragment size distribution. *Propellants, Explosive, Pyrotechnics, vol. 12.5, pp 175-178, 1987*

[36] Brown, Wilbur K., A Theory of Sequential Fragmentation and its application in Astronomical Application. *Journal of Astrophysics and Astronomy, vol. 10.1, pp 89-112, 1989*

[37] Elek, Predrag, and Slobodan Jaramaz., Size Distribution of Fragments Generated by Detonation of Fragmenting Warhead. *FME Transactions, vol. 37, no 3, 2009*

[38] Elek, Predrag, and Slobodan Jaramaz.,Fragment Size Distribution in Dynamic Fragmentation: Geometric Probability Approach. *FME Transactions, vol. 36, no 2, 2008*

[39] Gurney, Ronald W *The Initial Velocities of Fragments from Bomb, Shell and Grenades, BRL-405*. Army Ballistic Research Lab Aberdeen Proving Ground MD, 1943

[40] Rotariu, Adrian, and Eugen Trana., *Modeling and Simulation for Ballistic Protection*. Journal of Military Technical Academy, Bucharest, Romania, 2015

[41] Eshbach, Ovid Wallace, and Byron D. Tapley *Eshbach's handbook of engineering fundamentals*. John Wiley & Sons, 1990

[42] Szmelter, Joanna, and Chung Kiat Lee.,Prediction of Fragments Distribution and Trajectories of Exploding shells. *Journal of Battlefield Technology, vol. 10, no 2, 2007*

[43] Catovic, Alan, Berko Zecevic, and Jasmin Terzic,Analysis of Terminal Effectiveness For Several Types of HE Projectile and Impact Angles Using Coupled Numerical CAD Technique. *12th Seminar on New Trends in Research of Energetic Materials. 2009*

[44] Gilvarry, J. J, Fracture of brittle solids: Distribution function for fragment size in single fracture (Theoretical). *Journal of Applied Physics, vol. 32, pp 400-410, 1961*

[45] Zecevic, Berko, et al.,Characterization of distribution parameters of fragment mass and number for conventional projectiles. *New Trends in Research of Energetic Materials, Czech Republic, pp 1026-1039, 2011*

[46] Ugrcic, Marinko.,Numerical Simulation of fragmentation of High Explosive Projectiles. *Scientific Technical Review 63, vol. no 2, pp 47-57, 2013*